

Dissimilatory sulfate reduction in the archaeon 'Candidatus Vulcanisaeta moutnovskia' sheds light on the evolution of sulfur metabolism

Chernyh, Nikolay A.; Neukirchen, Sinje; Frolov, Evgenii N.; Sousa, Filipa L.; Miroshnichenko, Margarita L.; Merkel, Alexander Y.; Pimenov, Nikolay V.; Sorokin, Dimitry Y.; Ciordia, Sergio; Mena, Maria Carmen; Ferrer, Manuel; Golyshin, Peter; Lebedinsky, Alexander V.; Cardoso Pereira, Ines A.; Bonch-Osmolovskaya, Elizaveta A.

**Nature Microbiology**

DOI:  
[10.1038/s41564-020-0776-z](https://doi.org/10.1038/s41564-020-0776-z)

Published: 01/11/2020

Peer reviewed version

[Cyswllt i'r cyhoeddiad / Link to publication](#)

*Dyfyniad o'r fersiwn a gyhoeddwyd / Citation for published version (APA):*

Chernyh, N. A., Neukirchen, S., Frolov, E. N., Sousa, F. L., Miroshnichenko, M. L., Merkel, A. Y., Pimenov, N. V., Sorokin, D. Y., Ciordia, S., Mena, M. C., Ferrer, M., Golyshin, P., Lebedinsky, A. V., Cardoso Pereira, I. A., & Bonch-Osmolovskaya, E. A. (2020). Dissimilatory sulfate reduction in the archaeon 'Candidatus Vulcanisaeta moutnovskia' sheds light on the evolution of sulfur metabolism. *Nature Microbiology*, 5(11), 1428-+. <https://doi.org/10.1038/s41564-020-0776-z>

#### **Hawliau Cyffredinol / General rights**

Copyright and moral rights for the publications made accessible in the public portal are retained by the authors and/or other copyright owners and it is a condition of accessing publications that users recognise and abide by the legal requirements associated with these rights.

- Users may download and print one copy of any publication from the public portal for the purpose of private study or research.
- You may not further distribute the material or use it for any profit-making activity or commercial gain
- You may freely distribute the URL identifying the publication in the public portal ?

#### **Take down policy**

If you believe that this document breaches copyright please contact us providing details, and we will remove access to the work immediately and investigate your claim.

1  
2  
3

## 1. Extended Data

<b>Figure #</b>	<b>Figure title</b> One sentence only	<b>Filename</b> This should be the name the file is saved as when it is uploaded to our system. Please include the file extension. i.e.: <i>Smith_ED_Fig1.jpg</i>	<b>Figure Legend</b> If you are citing a reference for the first time in these legends, please include all new references in the Online Methods References section, and carry on the numbering from the main References section of the paper.
<b>Extended Data Fig. 1</b>	The microbial community composition of Oreshek Spring	Extended_Data_Figure_1.eps	Analysis by high throughput sequencing of 16S rRNA gene fragments.
<b>Extended Data Fig. 2</b>	Growth of <i>Thermoproteus tenax</i> .	Extended_Data_Figure_2.eps	The error bars are SD from independent growth replicates (n=3).
<b>Extended Data Fig. 3</b>	Growth of <i>Caldivirga maquilingsensis</i> .	Extended_Data_Figure_3.eps	Error bars represent standard deviations from independent growth replicates (n = 3).
<b>Extended Data Fig. 4</b>	H <sup>35</sup> S <sup>-</sup> formation from <sup>35</sup> SO <sub>4</sub> <sup>-2</sup> the binary culture 768-28 and the cultures of hyperthermophilic Crenarchaeota strains earlier claimed to be capable of sulphate reduction, but without experimental evidence.	Extended_Data_Figure_4.eps	Error bars represent standard deviations of independent radioisotopic measurement experiments (n = 3).

<b>Extended Data Fig. 5</b>	Genes related to sulphate reduction.	Extended_Data_Figure_5.eps	The key sulphate reduction genes from genomes of selected sulphate reducing archaea (“Candidatus <i>V. moutnovskia</i> ”, <i>Caldivirga</i> sp. Obs2 and <i>A. fulgidus</i> ) and bacteria ( <i>D. vulgaris</i> Hildenborough and <i>A. degensii</i> ) are shown, as well as from genomes of archaea not capable of sulphate reduction ( <i>V. distributa</i> , <i>V. souniana</i> , <i>Caldivirga</i> sp. MU80, <i>Ca. Methanodesulfokores washburnensis</i> MDKW and unclassified Aigarchaeota JZ bin 15).
<b>Extended Data Fig. 6</b>	Proteomic analysis of the soluble fraction of cells in the binary culture.	Extended_Data_Figure_6.eps	Protein extraction was performed with a non-denaturing detergent. Only the 150 most abundant proteins of “Candidatus <i>V. moutnovskia</i> ” are shown. a. Binary culture grown on medium with yeast extract and sulphate as the electron acceptor. b. Binary culture grown on medium with yeast extract and elemental sulphur as the electron acceptor. Protein abundances in mol% were estimated from nemPAI values <sup>62</sup> . Data are shown as the mean of n = 2 independent experiments fitted into a model.
<b>Extended Data Fig. 7</b>	Proteomic analysis of the binary culture after protein extraction with denaturing detergent.	Extended_Data_Figure_7.eps	Only proteins of “Candidatus <i>V. moutnovskia</i> ” are shown. The binary culture was grown on medium with yeast extract and sulphate as the electron acceptor. Protein abundances in mol% were estimated from nemPAI values <sup>62</sup> . Data are shown as the mean of n = 3 independent experiments fitted into a model.
<b>Extended Data Fig. 8</b>	Phylogenetic analysis of AprAB.	Extended_Data_Figure_8.eps	Maximum likelihood phylogenetic reconstruction (LG+I+G4) of a. AprA and b. AprB proteins present in

			the selected dataset. Only support values above 50 are shown. The scale bar indicates number of substitutions per site
<b>Extended Data Fig. 9</b>	Phylogenetic analysis of Sat.	Extended_Data_Figure_9.eps	Maximum likelihood phylogenetic reconstruction (LG+I+G4) of Sat proteins within the selected dataset. Only non-parametric support values above 70 are shown. The scale bar indicates number of substitutions per site.
<b>Extended Data Fig. 10</b>	Phylogenetic analysis of HdrA-like proteins.	Extended_Data_Figure_10.eps	Maximum-likelihood reconstruction (LG+I+G4) of the HdrA-domain present in 1,391 non-redundant HdrA, QmoA and QmoB proteins. The “ <i>Candidatus V. moutnovskia</i> ” sequences are marked in red. Expanded insets of the “ <i>Candidatus V. moutnovskia</i> ” QmoA (a) and QmoB (b) clades (marked in blue) are shown in Fig. 5. The scale bar indicates number of substitutions per site.

4

## 2. Supplementary Information:

5

6

### A. Flat Files

7

8

9

<b>Item</b>	<b>Present?</b>	<b>Filename</b> This should be the name the file is saved as when it is uploaded to our system, and should include the file extension. The extension must be .pdf	<b>A brief, numerical description of file contents.</b> i.e.: <i>Supplementary Figures 1-4, Supplementary Discussion, and Supplementary Tables 1-4.</i>
<b>Supplementary Information</b>	Yes	Supplementary_Informa	Supplementary Figure 1 and Supplementary Tables 1-3

		tion.pdf	
<b>Reporting Summary</b>	Yes	Report_Summary.pdf	

10  
11  
12  
13  
14

### B. Additional Supplementary Files

<b>Type</b>	<b>Number</b> If there are multiple files of the same type this should be the numerical indicator. i.e. "1" for Video 1, "2" for Video 2, etc.	<b>Filename</b> This should be the name the file is saved as when it is uploaded to our system, and should include the file extension. i.e.: <i>Smith_Supplementary_Video_1.mov</i>	<b>Legend or Descriptive Caption</b> Describe the contents of the file
Supplementary Table	Table S4	Supplementary_Table_4.xlsx	Genomic dataset used in the analysis including accession codes, taxonomic information and file location in the original database.

15  
16

### 3. Source Data

17  
18

Complete the Inventory below for all Source Data files.

19  
20

<b>Figure</b>	<b>Filename</b> This should be the name the file is saved as when it is uploaded to our system, and should include the file extension. i.e.: <i>Smith_SourceData_Fig1.xls</i> , or <i>Smith_Unmodified_Gels_Fig1.pdf</i>	<b>Data description</b> i.e.: Unprocessed Western Blots and/or gels, Statistical Source Data, etc.

Source Data Fig. 1	Source_Data_Figure1.xlsx	Binary Culture Growth source data
Source Data Fig. 2	Source_Data_Figure2.xlsx	Protein accessions of the hits underlying each symbol in figure 2.
Source Data Extended Data Fig. 2	Source_Data_Extended_Figure_2.xlsx	Raw data and calculations supporting Extended Data Figure 2
Source Data Extended Data Fig. 3	Source_Data_Extended_Figure_3.xlsx	Raw data and calculations supporting Extended Data Figure 3
Source Data Extended Data Fig. 4	Source_Data_Extended_Figure_4.xlsx	Raw data and calculations supporting Extended Data Figure 4
Source Data Extended Data Fig. 5	Source_Data_Extended_Figure_5.xlsx	Raw data and calculations supporting Extended Data Figure 5
Source Data Extended Data Fig. 6	Source_Data_Extended_Figure_6.xlsx	Raw data and calculations supporting Extended Data Figure 6
Source Data Extended Data Fig. 7	Source_Data_Extended_Figure_7.xlsx	Raw data and calculations supporting Extended Data Figure 7

21  
22  
23  
24  
25  
26  
27  
28  
29  
30  
31  
32  
33  
34  
35  
36  
37  
38  
39  
40  
41  
42  
43  
44  
45  
46  
47  
48  
49  
50  
51

# **Dissimilatory sulphate reduction in archaeon *Candidatus Vulcanisaeta moutnovskia* sheds light on evolution of sulphur metabolism**

Nikolay A. Chernyh<sup>1\*</sup>, Sinje Neukirchen<sup>2</sup>, Evgenii N. Frolov<sup>1</sup>, Filipa L. Sousa<sup>2\*</sup>, Margarita L. Miroshnichenko<sup>1</sup>, Alexander Y. Merkel<sup>1</sup>, Nikolay V. Pimenov<sup>1</sup>, Dimitry Y. Sorokin<sup>1</sup>, Sergio Ciordia<sup>3</sup>, María Carmen Mena<sup>3</sup>, Manuel Ferrer<sup>4</sup>, Peter N. Golyshin<sup>5</sup>, Alexander V. Lebedinsky<sup>1</sup>, Inês A. Cardoso Pereira<sup>6\*</sup>, Elizaveta A. Bonch-Osmolovskaya<sup>1,7</sup>

<sup>1</sup>Winogradsky Institute of Microbiology, Federal Research Center of Biotechnology, Russian Academy of Sciences, Leninsky prospect 33 Bldg 2, 119071, Moscow, Russia

<sup>2</sup>Archaea Biology and Ecogenomics Unit, Department of Functional and Evolutionary Ecology, University of Vienna, Althanstrasse 14 UZA I, 1090 Vienna, Austria

<sup>3</sup>Proteomics Facility, Centro Nacional de Biotecnología, CSIC, Madrid, Spain

<sup>4</sup>Institute of Catalysis, CSIC, Madrid, Spain

<sup>5</sup>School of Biological Sciences, Bangor University, Gwynedd LL57 2UW, UK

<sup>6</sup>Instituto de Tecnologia Química e Biológica António Xavier, Universidade Nova de Lisboa, Av. da República, 2780-157 Oeiras, Portugal

<sup>7</sup>Lomonosov Moscow State University, Faculty of Biology, 1-12 Leninskie Gory, 119991, Moscow, Russia

\*Corresponding authors: [chernyh3@yandex.com](mailto:chernyh3@yandex.com), [filipa.sousa@univie.ac.at](mailto:filipa.sousa@univie.ac.at) and [ipereira@itqb.unl.pt](mailto:ipereira@itqb.unl.pt)



53

54

55 **Abstract**

56

57 **Dissimilatory sulphate reduction (DSR), an important reaction in the biogeochemical**  
58 **sulphur cycle, has been dated to the Paleoproterozoic using geological evidence, but its**  
59 **evolutionary history is poorly understood. Several lineages of Bacteria carry out DSR but**  
60 **in archaea only *Archaeoglobus*, which acquired DSR genes from Bacteria, has been proven**  
61 **to catalyse this reaction. We investigated substantial rates of sulphate reduction in acidic**  
62 **hyperthermal terrestrial springs of the Kamchatka Peninsula and attributed DSR in this**  
63 **environment to Crenarchaeota in the *Vulcanisaeta* genus. Community profiling, coupled**  
64 **with radioisotope and growth experiments and proteomics, confirmed DSR by “*Candidatus***  
65 ***Vulcanisaeta moutnovskia*”, which has all the required genes. Other cultivated**  
66 **Thermoproteaceae were briefly reported to use sulphate for respiration but we were**  
67 **unable to detect DSR in these isolates. Phylogenetic studies suggest that DSR is rare in**  
68 **archaea and that it originated in *Vulcanisaeta*, independently of *Archaeoglobus*, by separate**  
69 **acquisition of *qmoABC* genes phylogenetically related to bacterial *hdrA* genes.**

70

71

72

73

## 74 **Introduction**

75 Microbial dissimilatory sulphate reduction (DSR) is the main driver of the modern sulphur cycle,  
76 and an important actor in the carbon cycle<sup>1,2</sup>. Although dissimilation of sulphur compounds was  
77 present on the early Earth<sup>3</sup>, there is dispute regarding the onset of DSR. The Paleoproterozoic barite  
78 deposits of 3.5, 3.4 and 3.2 Ga in Western Australia, India and South Africa support a well-  
79 mixed, large scale, marine sulphate pool<sup>4</sup>, with low micromolar concentrations<sup>5,6</sup>. This sulphate  
80 was produced by atmospheric photolysis of volcanic SO<sub>2</sub><sup>7</sup> and, as observed in modern  
81 environments<sup>8,9</sup>, the low levels of sulphate did not preclude active DSR. However, this  
82 metabolism did not imprint a strong mass-dependent fractionation on Archean sedimentary  
83 records probably due to a low level of biological activity and an atmospherically-derived  
84 elemental sulphur pool that masked isotopic evidence for DSR<sup>10</sup>. Nevertheless, the isotopic and  
85 microfossil evidence for Paleoproterozoic DSR<sup>11,12</sup> has been confirmed by recent high-resolution  
86 quadruple sulphur isotope measurements<sup>4,6,13</sup>, strongly supporting the existence of sulphate-  
87 reducing organisms at 3.55 Ga. However, the evolutionary history of sulphate reducers is poorly  
88 understood.

89 DSR capacity is found in several phyla of Bacteria, including Proteobacteria, Firmicutes,  
90 Thermodesulfobacteria, and Nitrospirae<sup>1</sup>, and possibly also in newly identified uncultured  
91 lineages<sup>14-18</sup>. Among Archaea, DSR has been reported in the hyperthermophilic marine  
92 *Archaeoglobus* genus of the Euryarchaeota, and for some hyperthermophilic terrestrial members  
93 of the Thermoproteaceae family from the Crenarchaeota, including *Caldivirga maquilingensis*<sup>19</sup>,  
94 *Vulcanisaeta distributa*<sup>20</sup>, *Vulcanisaeta souniana*<sup>20</sup>, *Thermoproteus tenax*<sup>21</sup>, and *Thermoproteus*  
95 *thermophilus*<sup>22</sup>. However, conclusive experimental proof of DSR, namely quantitative data on  
96 sulphide accumulation from growth with sulphate, has not been reported for the  
97 Thermoproteaceae. DSR is mediated by a specific set of proteins, which include sulphate  
98 adenylyl transferase (Sat), adenosine phosphosulphate reductase (AprAB) and the QmoABC  
99 membrane complex essential for sulphate reduction to sulphite<sup>23,24</sup>, as well as the dissimilatory  
100 sulphite reductase (DsrAB), its substrate DsrC, and the membrane DsrMK(JOP) complex,  
101 involved in sulphite reduction to sulphide<sup>24,25</sup>. The presence of DSR in both Archaea and  
102 Bacteria could indicate an ancient origin for this metabolism<sup>26</sup>. However, phylogenetic analyses  
103 of *Archaeoglobus aprAB* and *dsrAB* genes suggest their acquisition via horizontal gene transfer  
104 (HGT) from Bacteria<sup>27,28</sup>. In contrast, the Thermoproteaceae *dsrAB* genes represent a deep  
105 archaeal lineage distinct from bacterial sulphate reducers and sulphur oxidisers, supporting the  
106 origin of DsrAB as a reductive enzyme<sup>14,16,26,27</sup>. Thus, the Thermoproteaceae need to be further  
107 investigated to elucidate the evolutionary history of DSR.

108 Here, we studied terrestrial thermal acidic environments in which DSR was previously  
109 detected<sup>29</sup>. Using community profiling, culture studies and radioisotope measurements, coupled  
110 with comparative genomics, proteomics, and phylogenetics, we conclude that among the  
111 reported archaeal sulphate reducers with sequenced genomes, only *Archaeoglobus* spp. and  
112 “*Candidatus Vulcanisaeta moutnovskia*” are capable of DSR. In “*Candidatus V. moutnovskia*”  
113 (as in *Archaeoglobus* spp.) this activity correlates with the presence of functional (full-length)  
114 *qmoABC* genes, which are absent or truncated in the genomes of other Thermoproteaceae.  
115 Furthermore, the *qmoABC* genes of “*Candidatus V. moutnovskia*” and *Archaeoglobus* spp. are  
116 of different evolutionary origin (albeit in both cases bacterial). These observations suggest that  
117 DSR arose twice in archaea, both times by acquisition of bacterial genes, and seems to be  
118 dependent on functional *qmoABC* genes needed for energy conservation. In contrast,  
119 dissimilatory sulphite reduction appears to be more ancient and may have arisen early within the  
120 Thermoproteaceae.

121

### 122 **Community profiling of Oreshek Spring**

123 The microbial community of Oreshek Spring (Moutnovsky Volcano, Kamchatka Peninsula,  
124 Russia, temperature of 91°C, pH 3.5, sulphate concentration of 538 mg/l), which displays  
125 significant rates of sulphate reduction (1.094 nmol H<sub>2</sub>S/cm<sup>3</sup>·day)<sup>29</sup>, was analysed by sequencing  
126 16S rRNA gene fragments. After quality filtering, we obtained 28152716S rRNA gene  
127 fragments corresponding to 434 operational taxonomic units (OTUs) defined with 0.98 similarity  
128 threshold. This allowed a coverage of 0.825 for the microbial community, estimated by  
129 determining Chao1 richness (Chao1=526). Such coverage does not permit a complete description  
130 of phylogenetic diversity, but allows identification of all major groups. The prokaryotic diversity  
131 in Oreshek Spring was estimated by the Shannon index, which amounted to 3.37. Archaea  
132 dominated the microbial community, accounting for 85.0% of 16S rRNA genes obtained.  
133 Bacterial sequences accounted for 13.0%, and 2.0% of sequences could not be affiliated. The  
134 archaeal sequences represented three phyla: Crenarchaeota (75% of all library sequences),  
135 Thaumarchaeota (2.0%) and Euryarchaeota (8.0%). Among the archaeal representatives, three  
136 genera of putative sulphate reducers were detected: *Vulcanisaeta*, *Thermoproteus* and *Caldivirga*  
137 (20.0%, 9.0% and 0.9% of library sequences). Among bacterial sequences, no taxa representing  
138 known sulphate reducers were detected. Thus, sulphate reduction at Oreshek Spring seems to be  
139 performed mainly by archaea, among which *Vulcanisaeta* spp. predominate (**Extended Data**  
140 **Figure 1**).

141 Two sulphate-reducing cultures were previously enriched from hot springs at  
142 Moutnovsky Volcano, both containing archaea of the genera *Vulcanisaeta* and *Thermoproteus*.

143 The *Vulcanisaeta* component of culture 768-28 was given the tentative species name  
144 “*Candidatus V. moutnovskia*”<sup>29-31</sup>. We designed specific primers for the detection of  
145 “*Candidatus V. moutnovskia*” *dsrAB* genes and used them for qPCR analysis of an  
146 environmental sample from Oreshek Spring. The primers specificity was confirmed by amplicon  
147 sequencing. A significant number of “*Candidatus V. moutnovskia*” *dsrAB* genes were detected  
148 (**Supplementary Table 1**). In the same sample, we assessed the abundance of archaea and  
149 bacteria using qPCR with 16S rRNA gene-specific primers. Comparison of the qPCR results  
150 with 16S rDNA- and *dsrAB*-specific primers showed that archaea represented 95% of all  
151 prokaryotes in the community, and of them, 40% were archaeal sulphate reducers related to  
152 “*Candidatus V. moutnovskia*” (**Supplementary Table 1**).

153

### 154 **Sulphate reduction by Crenarchaeota**

155 For studies of DSR we used the binary culture 768-28<sup>30</sup> (hereafter referred to as the binary  
156 culture), which contains “*Candidatus V. moutnovskia*” and *Thermoproteus uzoniensis* (all  
157 attempts to isolate the pure cultures were unsuccessful). Using liquid medium with sulphate as  
158 electron acceptor and yeast extract as energy source, we tested the DSR capacity of the binary  
159 culture and of the pure cultures of putative Thermoproteaceae sulphate reducers *T. tenax*, *V.*  
160 *distributa*, *V. souniana*, and *C. maquilingensis*. The binary culture was able to grow by DSR  
161 with yeast extract, showing sulphate consumption and sulphide accumulation (**Fig. 1**). Among  
162 tested electron donors, only peptone and yeast extract supported growth with sulphate  
163 (**Supplementary Table 2**). In sulphate-reducing conditions “*Candidatus V. moutnovskia*”  
164 predominated in the binary culture, while *T. uzoniensis* was present only as a minor component.  
165 qPCR with 16S rRNA gene-specific primers showed that in DSR conditions the share of *T.*  
166 *uzoniensis* was 0.01 to 0.1%, while in sulphur-reducing conditions it increased to 50%. This  
167 suggests that DSR is a capacity of “*Candidatus V. moutnovskia*”, while *T. uzoniensis* is likely  
168 incapable of sulphate reduction, as supported by genomic and proteomic analyses (see below).

169 Cultures of *T. tenax*, *V. distributa*, *V. souniana* and *C. maquilingensis*, obtained from  
170 validated collections, showed good growth on medium with elemental sulphur as electron  
171 acceptor (authenticity of the grown cultures was checked by 16S rRNA gene sequencing), but no  
172 growth by DSR with any electron donor (**Supplementary Table 2**). Neither consumption of  
173 sulphate nor accumulation of sulphide were observed after 10 days of incubation, and there was  
174 either no increase in cell number or sometimes only a very slight increase (2-fold). This could be  
175 due to a small amount of sulphur formed from oxidation of sulphide used as medium reductant,  
176 or a small growth stimulation due to assimilation of sulphate. The former hypothesis was  
177 confirmed in further experiments where similar small biomass increments were produced in the

178 presence of sulphate and in the absence of externally added electron acceptors (**Extended Data**  
179 **Figure 2 and Extended Data Figure 3**).

180 To test the ability for DSR with higher sensitivity, we used the radioisotopic approach to  
181 measure sulphate reduction in these Thermoproteaceae (**Extended Data Figure 4**). Using the  
182 cell numbers at the end of incubation, we calculated the specific sulphate reduction rate by the  
183 “*Candidatus V. moutnovskia*” culture to be 1.055 fmol sulphate cell<sup>-1</sup> day<sup>-1</sup>. This value falls  
184 within the range of 0.16–417 fmol sulphate cell<sup>-1</sup> day<sup>-1</sup> reported for pure cultures of sulphate  
185 reducers<sup>32,33</sup>, while the specific sulphate reduction rates for *T. tenax*, *V. distributa*, *V. souniana*,  
186 and *C. maquilingensis* were negligible. Thus, of the five organisms tested, only “*Candidatus V.*  
187 *moutnovskia*” seems to be capable of DSR.

188

### 189 **Sulphate reduction gene distribution in archaea**

190 The previously sequenced “*Candidatus V. moutnovskia*” genome<sup>31</sup> contains the minimal set of  
191 genes necessary for DSR, namely genes for sulphate transporters and pyrophosphatase, *sat*,  
192 *aprAB*, *qmoABC*, *dsrAB*, *dsrC* and *dsrMK*. In addition, we found no evidence for possible  
193 alternative genes that could be involved in this process, such as coding for membrane complexes  
194 or HdrA-related proteins (with one exception, see below). This analysis was extended to a large  
195 (meta)genomic dataset which showed that, apart from *Archaeoglobus* spp. and “*Candidatus V.*  
196 *moutnovskia*” no other archaeon possesses a complete set of full-length genes necessary for  
197 DSR (**Fig. 2 and Extended Data Figure 5**). Among the Thermoproteaceae cultures claimed to  
198 be capable of DSR, *T. tenax*, *V. distributa* and *C. maquilingensis* lack the *qmoABC* genes, and *T.*  
199 *tenax* and *C. maquilingensis* also contain no *hdrA*-like genes. In the *V. souniana* low quality  
200 draft genome, all necessary genes for DSR could be found, but several of them appear to be  
201 impaired (with an apparent abundance of sequencing artefacts masking possible natural  
202 frameshifts). In the genome of *T. uzoniensis*, the second component of the binary culture, the  
203 *dsrAB*, *dsrMK*, and *qmoABC* genes are absent, while *sat*, *aprAB* and *dsrC* are present.

204 Recently, the presence of *dsrABC* genes has been reported in several uncultivated  
205 organisms belonging to the Aigarchaeota<sup>17,34</sup>, Korarchaeota<sup>16</sup> and Hydrothermarchaeota<sup>15</sup>  
206 candidate phyla. We found that in *Candidatus* Hydrothermarchaeota genomes, no *qmoABC* or  
207 bona-fide *aprAB* could be identified, although bona fide *sat*, *dsrABC* and *dsrMK* are present.  
208 Interestingly, in both *Ca. Methanodesulfokores washburnensis* MDKW and uncultivated  
209 Aigarchaeota JZ bin 15 genomes, in which the presence of *dsrAB*, *dsrC* and *dsrMK* has been  
210 reported<sup>17</sup>, *qmoABC* gene candidates were also found, albeit no *aprAB* genes were present (**Fig.**  
211 **2**). Both metagenomic assemblies have a high level of completeness (above 95%), but it cannot  
212 be excluded that *aprAB* genes are located in the missing part of the assembly. Similar *qmoABC*

213 homologues were also identified in genomes lacking any *dsr* genes, such as in the complete  
214 genome of *Ca. Korarchaeum cryptofilum* OPF8 (**Fig. 2**). None of the Asgard lineages, in which  
215 Thorarchaeota genomes are included, have the *dsr* genes required for dissimilatory  
216 sulphate/sulphite reduction.

217

### 218 **Proteomics of the binary culture**

219 We performed proteomic analysis of the binary culture grown anaerobically with sulphate or  
220 sulphur as electron acceptors (**Extended Data Figure 6**). For cells grown with sulphate, several  
221 of the most abundant proteins detected were “*Candidatus V. moutnovskia*” proteins involved in  
222 sulphate reduction (**Supplementary Table S3**), whereas no *T. uzoniensis* proteins that might be  
223 involved in sulphate reduction (Sat, AprAB and DsrC) could be identified. The “*Candidatus V.*  
224 *moutnovskia*” QmoAB proteins were detected only in DSR conditions, as well as a related  
225 protein with a domain composition similar to a fusion of QmoA and QmoB (“QmoAB-like”,  
226 VMUT\_0635). The latter protein is a distant relative of *Geobacter metallireducens* BamE, a  
227 subunit of the Benzoyl CoA-reductase<sup>35</sup>, and is not conserved in other sulphate reducers (or in *T.*  
228 *tenax*, *V. souniana* and *C. maquilingensis*, while it is present in *V. distributa*, which is also not a  
229 sulphate reducer), so it is unlikely to be involved in DSR. There are no other HdrA-related  
230 proteins encoded in the genome of “*Candidatus V. moutnovskia*”. In contrast, no sulphate  
231 reduction proteins were detected for cells grown with sulphur.

232 A second proteomic analysis of the sulphate-grown culture was performed to try to  
233 increase the detection of membrane proteins, by extracting proteins with a denaturing detergent  
234 (**Extended Data Figure 7, Supplementary Table S3**). This second analysis allowed the  
235 detection of “*Candidatus V. moutnovskia*” DSR-related membrane proteins (QmoABC, DsrMK,  
236 proton-pumping pyrophosphatase and a sulphate transporter). We found no evidence of other up-  
237 regulated proteins in “*Candidatus V. moutnovskia*” whose involvement in sulphate reduction  
238 would be conceivable. Thus, the proteomic results confirmed that DSR by the binary culture was  
239 performed by “*Candidatus V. moutnovskia*”, and showed that several of the proteins involved  
240 are among the most highly expressed proteins in cells grown by this mode.

241

242

### 243 **Phylogenetic analysis of archaeal sulphate reduction**

244 We performed a phylogenetic analysis of key genes specific for sulphate reduction, *sat*, *aprAB*  
245 and *qmoAB(C)*, to investigate the evolutionary history of DSR. Detailed phylogenetic studies  
246 were already reported for *dsrAB*<sup>14,16,26,27,36</sup>, indicating the ancient presence or origin of these  
247 genes within the Thermoproteaceae, associated with dissimilatory sulphite reduction.

248 In the *aprA* single gene phylogenies (**Fig. 3 and Extended Data Figure 8**), two highly  
249 supported clades are observed, one containing bona-fide *aprA* genes, and another composed of  
250 *aprA*-like homologues belonging to different lineages. The *aprA*-like sequences belong to  
251 organisms that are not dissimilatory sulphate reducers/sulphur oxidisers or that have a bona-fide  
252 *aprA* gene (**Fig. 3 and Extended Data Figure 8a**). These genes probably correspond to proteins  
253 with a different and unknown function. Within the AprA clade, the separation of Crenarchaeota  
254 and sulphur oxidisers proteobacterial group II from Bacteria/*Archaeoglobus* and sulphur  
255 oxidisers proteobacterial group I is highly supported, as previously reported<sup>28,37,38</sup>. Group I  
256 sulphur oxidisers, including purple sulphur bacteria, have AprM as physiological partner of  
257 AprAB and show an *aprAB* phylogeny mostly congruent with *dsrAB*, whereas Group II sulphur  
258 oxidisers and green sulphur bacteria, which have QmoABC as physiological partner of AprAB,  
259 apparently acquired the *aprAB* genes from sulphate reducers. Due to the small length of the  
260 alignment (163 positions after trimming), the *aprB* phylogeny has many unresolved branches  
261 (**Extended Data Figure 8b**), but the general trends observed in the *aprA* phylogeny are retained.  
262 The phylogenetic position of the Thermoproteaceae *aprAB* may indicate the ancient origin of  
263 these genes in this family, or their acquisition/replacement by an HGT event between this lineage  
264 and an ancestor of the group I sulphur oxidisers.

265 The *sat* gene presents an even more complex evolutionary history (**Extended Data**  
266 **Figure 9**), probably due to its possible role in either assimilatory or dissimilatory sulphate  
267 reduction. Indeed, in the *sat* single gene tree Bacteria are not monophyletic and evidence for  
268 several recent interdomain HGT events is present.

269 The full-length *qmoABC* genes are absent in the Crenarchaeota, with the exception of  
270 “*Candidatus V. moutnovskia*” and the *Caldivirga* sp. Obs2 metagenomic assembly (**Figs. 2 and**  
271 **4**), suggesting a critical role of these genes in DSR. The three genes code for a membrane  
272 complex responsible for electron transfer from the menaquinol pool to APS reductase<sup>23,39</sup>  
273 (**Supplementary Figure 1**). QmoC oxidizes menaquinol, presumably with proton release to the  
274 periplasm, and electrons are transferred through the QmoC hemes *b* and Fe-S centers to QmoA  
275 and QmoB, which transfers them to APS reductase<sup>39</sup>. In bacteria, the QmoABC complex was  
276 shown to be essential for sulphate, but not sulphite, reduction<sup>40</sup>, and the corresponding genes are  
277 strictly conserved in sulphate reducers<sup>24,28</sup>, with the exception of *qmoC* in some clostridial  
278 organisms. In these organisms two *hdrBC* genes (in some *Desulfotomaculum* spp.) or *hdrD*  
279 genes (in some *Desulfosporosinus* spp.) are found instead, but these genes cannot functionally  
280 replace *qmoC* in energy conservation<sup>40</sup>, and their function is unknown. The QmoA and QmoB  
281 proteins are both related to the methanogenic HdrA, a subunit of heterodisulfide reductases<sup>41,42</sup>.  
282 However, QmoA and QmoB have very distinct physiological functions from HdrA proteins.

283 QmoA is smaller than HdrA and lacks some of its domains and [4Fe-4S] clusters, whereas  
284 QmoB has a similar size as HdrA, but also lacks some of its [4Fe-4S] clusters, having an  
285 additional C-terminal domain related to the electron transfer protein MvhD<sup>23</sup> (**Fig. 4**). The QmoC  
286 protein is distinct and has a cytochrome *b* membrane domain related to HdrE, and an electron-  
287 transfer iron-sulphur domain related to HdrC.

288 To understand the evolutionary relationship between *hdrA*, *qmoA* and *qmoB* genes (**Fig. 5**  
289 **and Extended Data Figure 10**), a large taxonomic sampling was performed. In this  
290 reconstruction “*Candidatus V. moutnovskia*” and *Caldivirga* sp. Obs2 QmoA are inside a  
291 bacterial clade, whose most basal sequence is the *Ammonifex degensii* QmoA2. This highly  
292 supported clade (**Fig. 5a**) is dominated by metagenomic sequences of uncharacterized HdrA-like  
293 proteins affiliated with Bacteroidetes (sister clade of “*Candidatus V. moutnovskia*” QmoA),  
294 Chloroflexi, Elusimicrobia and Deltaproteobacteria. The “*Candidatus V. moutnovskia*” QmoAB  
295 proteins show a close relationship to QmoAB2 from *A. degensii*, a bacterium that has two  
296 *qmoABC* gene clusters. Surprisingly, the “*Candidatus V. moutnovskia*” QmoAB and *Ammonifex*  
297 QmoAB2 are more closely related to bacterial HdrA proteins than to canonical QmoAB proteins  
298 from Bacteria/*Archaeoglobus* (which include the QmoAB1 from *A. degensii*) (**Extended Data**  
299 **Figure 10**). The closer proximity between “*Candidatus V. moutnovskia*” branches and *A.*  
300 *degensii* is associated with (or reflects) the presence of two additional [4Fe-4S] clusters in both  
301 QmoA and QmoB from *Vulcanisaeta* and *Ammonifex*, as well as the presence of an additional  
302 domain (the “inserted ferredoxin domain”<sup>42</sup>, absent in bacterial QmoB) and the absence of the C-  
303 terminal MvhD domain in *Vulcanisaeta* and *Ammonifex* QmoB, which is encoded in a separate  
304 gene upstream of *Vulcanisaeta qmoA* (**Fig. 4**). The “*Candidatus V. moutnovskia*” QmoC protein  
305 is more similar to *A. degensii* QmoC1 than to QmoC2, contrary to what might be expected since  
306 its QmoAB are more closely related to *Ammonifex* QmoAB2, suggesting a *qmoC* acquisition  
307 event separate from the acquisition of *qmoAB* (**Extended Data Figure 5**). Twelve archaeal  
308 sequences from mainly uncultivated organisms are basal to the *Vulcanisaeta* and *Ammonifex*  
309 QmoA clade that has bona-fide methanogenic HdrA as sister (**Extended Data Figure 10**).  
310 However, the low support of these twelve archaeal sequences does not allow to resolve with  
311 confidence their exact position within the phylogenetic reconstruction.

312 The “*Candidatus V. moutnovskia*” QmoB clade is very similar to the QmoA clade (in  
313 terms of topology and taxonomic affiliations of their OTUs), wherein “*Candidatus V.*  
314 *moutnovskia*” and *Caldivirga* sp. Obs2 QmoB are also inside a highly supported and resolved  
315 bacterial clade with *A. degensii* QmoB2 sequence being basal (**Fig. 5b**). Similarly to QmoA, an  
316 HdrA-like archaeal clade with very similar taxonomic distribution of uncultivated organisms is  
317 at the base of the “*Candidatus V. moutnovskia*” QmoB bacterial clade but, this time, descending

318 from metagenomic Deltaproteobacteria, which is an indication of interdomain HGT. Although  
319 having a higher statistical support, the exact position of these sequences cannot be fully resolved.

320 The phylogenetic reconstruction of HdrA-like proteins (**Fig. 5 and Extended Data**  
321 **Figure 10**) points to the acquisition of the “*Candidatus V. moutnovskia*” *qmoAB* genes from a  
322 bacterial donor. The nature of the primordial organisms in which the transition from an HdrA to  
323 a QmoA/B protein occurred is not clear. Until some of these organisms are cultivated, Occam’s  
324 razor suggests the bacterial affiliation of this transition since in both *Vulcanisaeta* QmoA/B  
325 clades, the most basal organism known to perform sulphate reduction is *A. degensii*, and in many  
326 of the archaeal lineages basal to the clade there is no evidence for the ability for sulphate or  
327 sulphite reduction. Overall, this data suggests that “*Candidatus V. moutnovskia*” “re-invented”  
328 DSR by acquiring QmoAB proteins from a bacterial organism, where the separate evolution of  
329 Qmo proteins from a typical HdrA took place, and, thus, extant DSR in Thermoproteaceae has  
330 an independent evolutionary history from that in Bacteria and *Archaeoglobus* species.

331

## 332 **DISCUSSION**

333 The evolutionary history of DSR is poorly understood, particularly among the archaea. Sulphate is  
334 present in high-temperature submarine, deep subsurface and terrestrial environments where  
335 archaeal organisms are abundant. Several independent studies have reported high-temperature  
336 sulphate reduction in terrestrial neutral or acidic hot springs of Yellowstone National Park<sup>43</sup> and  
337 Kamchatka Peninsula<sup>29,44,45</sup>, but the species responsible for high-temperature sulphate reduction  
338 had not been identified. We report that hyperthermophilic archaea of the genus *Vulcanisaeta* are  
339 one of the dominant groups in the acidic and hot Oreshek Spring. Using growth, radioisotopic,  
340 and proteomic experiments with the binary culture 768-28, we show that “*Candidatus V.*  
341 *moutnovskia*” is responsible for sulphate reduction, while *T. uzoniensis* is only a minor  
342 component in DSR conditions, with its share growing only upon growth with elemental sulphur.  
343 Furthermore, the DSR capacity briefly reported for other four Thermoproteaceae species (*T.*  
344 *tenax*, *C. maquilingensis*, *V. distributa* and *V. souniana*) could not be confirmed in detailed  
345 growth and radioisotopic studies. No quantitative data was provided in any of these previous  
346 studies and the weak growth observed with sulphate was probably not statistically different from  
347 the weak growth without any electron acceptor, a possibility that we confirmed (**Supplementary**  
348 **Table 2, and Extended Data Figure 2 and Extended Data Figure 3**).

349 Our observations on DSR ability by the Thermoproteaceae may be explained through  
350 genomic analyses of available complete archaeal genomes: the minimal set of genes shown to be  
351 required for DSR in bacteria<sup>24,40</sup> was only found in the genomes of *Archaeoglobus* spp. and  
352 “*Candidatus V. moutnovskia*”. Notably, with the exception of *Caldivirga* sp. Obs2, the other

353 Thermoproteaceae investigated had the *sat*, *aprAB* and *dsrABCMK* genes, but lacked the  
354 *qmoABC* genes. The QmoABC respiratory complex<sup>23</sup> was shown to be essential for growth of a  
355 sulphate reducing bacterium on sulphate, but not on sulphite<sup>40</sup>, and seems to allow energy  
356 conservation during the step of APS reduction. The alternative *aprM* present in sulphur oxidisers  
357 (or the *hdrBC* genes in clostridial sulphate reducers), are also absent in Thermoproteaceae. These  
358 results suggest that DSR by “*Candidatus V. moutnovskia*” is associated with the acquisition of  
359 the *qmoABC* genes by HGT, whereas other Thermoproteaceae may only reduce sulphate for  
360 assimilatory purposes, as they lack the QmoABC complex that would enable them to conserve  
361 energy from that reduction.

362 Phylogenetic analyses show that the “*Candidatus V. moutnovskia*” *dsr* genes, like those  
363 of other Thermoproteaceae, are rooted in the Archaea domain, contrary to *dsr* genes of  
364 *Archaeoglobus* spp., which were acquired from bacterial lineages<sup>14,16,26,27</sup>. In contrast, the  
365 “*Candidatus V. moutnovskia*” *qmoABC* genes have a distinct evolutionary history. The *qmoAB*  
366 genes, together with the bacterial *A. degensii qmoAB2* genes and genes of other bacterial  
367 organisms from the same clade, are more closely related to typical *hdrA* genes, than to bacterial  
368 *qmoAB* genes. Thus, the “*Candidatus V. moutnovskia*” *qmo* genes are not derived from  
369 canonical *qmo* genes from Bacteria, but are apparently the result of a separate functional  
370 evolution directly from bacterial *hdrA* genes. This indicates that the acquisition of the *qmoAB(C)*  
371 genes by “*Candidatus V. moutnovskia*”, apparently conferring DSR capacity to this organism,  
372 may have been a more recent event than their ability to perform dissimilatory sulphite and/or  
373 assimilatory sulphate reduction.

374 These results have important implications for understanding the evolution of  
375 dissimilatory sulphur metabolism, and three evolutionary scenarios can be considered. The first  
376 is that assimilatory or dissimilatory sulphite reduction was already present before the archaeal-  
377 bacterial divide. This agrees with the proposed existence of an assimilatory or dissimilatory  
378 enzyme for sulphite reduction in ancestral organisms, either prior to the divergence of the  
379 bacterial and archaeal domains<sup>46</sup> or early after the archaeal-bacterial division followed by an  
380 interdomain transfer. In this scenario, dissimilatory sulphite reduction was subsequently lost in  
381 most archaeal lineages, being only retained in a single Crenarchaeota family. Later interdomain  
382 HGTs events would be responsible for the presence of dissimilatory sulphite reduction in other  
383 archaeal lineages<sup>16,17</sup>. The second scenario is that dissimilatory sulphite reduction originated  
384 within Archaea (Thermoproteaceae) and was acquired by Bacteria due to an early HGT event.  
385 Subsequently, several intradomain HGTs occurred expanding this trait across systematic  
386 boundaries. The presence of the *dsr* genes within several bacterial phyla would suggest a high  
387 number of such events. The third scenario is that dissimilatory sulphite reduction is of early

388 bacterial origin and Crenarchaeota acquired the *dsr* genes by an early HGT to the  
389 Thermoproteaceae ancestor. This scenario agrees with recent studies<sup>16,17,36</sup>, which indicate  
390 several independent archaeal acquisitions of dissimilatory sulphite reduction genes from bacteria.

391 In contrast, DSR has apparently a separate evolutionary history. It may have been  
392 preceded by assimilatory sulphate reduction, which could have been the initial physiological  
393 function of the AprAB enzyme, namely in the Thermoproteaceae, given the absence of AprM or  
394 QmoABC. In this scenario DSR evolved within the bacterial domain, presumably originating  
395 through the development of QmoABC proteins, and was only later transferred to a limited  
396 number of organisms in the Archaea, namely *Archaeoglobus* spp., “*Candidatus V.*  
397 *moutnovskia*” and *Caldivirga* sp. Obs2, of which at least the first two acquired QmoABC as  
398 independent evolutionary events. An alternative, less likely, hypothesis is that ancestors of the  
399 Thermoproteaceae were early archaeal dissimilatory sulphate reducers, which subsequently lost  
400 this ability, presumably by loss of the *qmoABC* (or *aprM* genes), that were re-acquired by  
401 “*Candidatus V. moutnovskia*” and *Caldivirga* sp. Obs2. The ancestry of dissimilatory sulphite  
402 over sulphate reduction makes sense from a bioenergetic point of view as ATP is required for  
403 sulphate, but not for sulphite, reduction, and also in terms of the different availability of the two  
404 compounds on the early Earth. In the anoxic, reduced Earth, sulphate was present at low  
405 concentration, produced from SO<sub>2</sub> photolysis<sup>7</sup>, or biologically from sulphide anoxygenic  
406 photosynthesis<sup>47</sup> or disproportionation of sulphur compounds. In contrast, sulphite produced  
407 from hydrolysis of volcanic and hydrothermal SO<sub>2</sub> was probably abundant. The evolutionary  
408 history of siroheme sulphite reductases also supports the ancestry of sulphite reduction<sup>46</sup>. Recent  
409 phylogenomic analysis of novel Diaforarchaea also endorse the view that most organisms with  
410 early-branching DsrAB are capable of sulphite, but not sulphate, reduction<sup>36</sup>.

411 In conclusion, assimilatory/dissimilatory sulphite reduction may have been present before  
412 the Bacteria/Archaea divide or shortly after, and likely preceded dissimilatory sulphate  
413 reduction. Nevertheless, DSR is an ancient process dating back at least to 3.5 Ga, which was  
414 likely restricted to Bacteria that were limited in biological activity by the low levels of sulphate.  
415 In the Thermoproteaceae, assimilatory sulphate reduction may have been an ancient trait and our  
416 results suggest that a later acquisition of the *qmoABC* genes allowed “*Candidatus V.*  
417 *moutnovskia*” to grow by reduction of sulphate. Nevertheless, further experimental studies of  
418 archaeal sulphate reduction are required to confirm this idea and firmly clarify the role of the  
419 *qmo* and *hdr* genes in archaea, as additional or different genes may be involved. At about 2.4 Ga,  
420 the rise in O<sub>2</sub> levels started the slow oxygenation of the oceans and atmosphere, with the  
421 associated increase in marine sulphate concentration. This process then led to the strong  
422 diversification of bacterial lineages capable of sulphate reduction, as observed today.

423 **References**

424

- 425 1. Rabus, R. *et al.* A Post-Genomic View of the Ecophysiology, Catabolism and  
426 Biotechnological Relevance of Sulphate-Reducing Prokaryotes. *Adv. Microb. Physiol.* **66**,  
427 55–321 (2015).
- 428 2. Wasmund, K., Mußmann, M. & Loy, A. The life sulfuric: microbial ecology of sulfur  
429 cycling in marine sediments. *Environ. Microbiol. Rep.* **9**, 323–344 (2017).
- 430 3. Canfield, D. E., Rosing, M. T. & Bjerrum, C. Early anaerobic metabolisms. *Philos. Trans.*  
431 *R. Soc. B Biol. Sci.* **361**, 1819–1836 (2006).
- 432 4. Roerdink, D. L., Mason, P. R. D., Farquhar, J. & Reimer, T. Multiple sulfur isotopes in  
433 Paleoarchean barites identify an important role for microbial sulfate reduction in the early  
434 marine environment. *Earth Planet. Sci. Lett.* **331–332**, 177–186 (2012).
- 435 5. Crowe, S. A. *et al.* Sulfate was a trace constituent of Archean seawater. *Science* **346**, 735–  
436 739 (2014).
- 437 6. Zhelezinskaia, I., Kaufman, A. J., Farquhar, J. & Cliff, J. Large sulfur isotope  
438 fractionations associated with Neoproterozoic microbial sulfate reduction. *Science* **346**, 742–  
439 744 (2014).
- 440 7. Farquhar, J., Bao, H. M. & Thiemens, M. Atmospheric influence of Earth’s earliest sulfur  
441 cycle. *Science* **289**, 756–758 (2000).
- 442 8. Loy, A., Kusel, K., Lehner, A., Drake, H. L. & Wagner, M. Microarray and functional  
443 gene analyses of sulfate-reducing prokaryotes in low-sulfate, acidic fens reveal  
444 cooccurrence of recognized genera and novel lineages. *Appl. Environ. Microbiol.* **70**, 6998–  
445 7009 (2004).
- 446 9. Leloup, J. *et al.* Diversity and abundance of sulfate-reducing microorganisms in the  
447 sulfate and methane zones of a marine sediment, Black Sea. *Environ. Microbiol.* **9**, 131–  
448 142 (2007).
- 449 10. Farquhar, J. *et al.* Pathways for Neoproterozoic pyrite formation constrained by mass-  
450 independent sulfur isotopes. *Proc. Natl. Acad. Sci. U. S. A.* **110**, 17638–17643 (2013).
- 451 11. Shen, Y., Buick, R. & Canfield, D. E. Isotopic evidence for microbial sulphate reduction  
452 in the early Archean era. *Nature* **410**, 77–81 (2001).
- 453 12. Wacey, D., Kilburn, M. R., Saunders, M., Cliff, J. & Brasier, M. D. Microfossils of  
454 sulphur-metabolizing cells in 3.4-billion-year-old rocks of Western Australia. *Nat. Geosci.*  
455 **4**, 698–702 (2011).
- 456 13. Ueno, Y., Ono, S., Rumble, D. & Maruyama, S. Quadruple sulfur isotope analysis of ca.  
457 3.5 Ga Dresser Formation: New evidence for microbial sulfate reduction in the early  
458 Archean. *Geochim. Cosmoch. Acta* **72**, 5675–5691 (2008).
- 459 14. Anantharaman, K. *et al.* Expanded diversity of microbial groups that shape the  
460 dissimilatory sulfur cycle. *ISME J.* **12**, 1715–1728 (2018).
- 461 15. Carr, S. A. *et al.* Carboxydrotrophy potential of uncultivated Hydrothermarchaeota from  
462 the seafloor crustal biosphere. *ISME J.* **13**, 1457–1468 (2019).
- 463 16. McKay, L. J. *et al.* Co-occurring genomic capacity for anaerobic methane and  
464 dissimilatory sulfur metabolisms discovered in the Korarchaeota. *Nat. Microbiol.* **4**, 614–  
465 622 (2019).
- 466 17. Hua, Z. S. *et al.* Genomic inference of the metabolism and evolution of the archaeal  
467 phylum Aigarchaeota. *Nat. Commun.* **9**, 2832 (2018).
- 468 18. Tan, S. *et al.* Insights into ecological role of a new deltaproteobacterial order *Candidatus*  
469 *Acidulodesulfobacterales* by metagenomics and metatranscriptomics. *ISME J.* **1** (2019).  
470 doi:10.1038/s41396-019-0415-y
- 471 19. Itoh, T., Suzuki, K., Sanchez, P. C. & Nakase, T. *Caldivirga maquilangensis* gen. nov., sp.  
472 nov., a new genus of rod-shaped crenarchaeote isolated from a hot spring in the  
473 Philippines. *Int. J. Syst. Bacteriol.* **49**, 1157–1163 (1999).
- 474 20. Itoh, T., Suzuki, K. I. & Nakase, T. *Vulcanisaeta distributa* gen. nov., sp. nov., and

- 475 *Vulcanisaeta souniana* sp. nov., novel hyperthermophilic, rod-shaped crenarchaeotes  
476 isolated from hot springs in Japan. *Int. J. Syst. Evol. Microbiol.* **52**, 1097–1104 (2002).
- 477 21. Siebers, B. *et al.* The complete genome sequence of *Thermoproteus tenax*: A  
478 physiologically versatile member of the Crenarchaeota. *PLoS One* **6**, e24222 (2011).
- 479 22. Yim, K. J., Song, H. S., Choi, J. S. & Roh, S. W. *Thermoproteus thermophilus* sp. nov., a  
480 hyperthermophilic crenarchaeon isolated from solfataric soil. *Int. J. Syst. Evol. Microbiol.*  
481 **65**, 2507–2510 (2015).
- 482 23. Pires, R. H. *et al.* A novel membrane-bound respiratory complex from *Desulfovibrio*  
483 *desulfuricans* ATCC 27774. *Biochim. Biophys. Acta - Bioenerg.* **1605**, 67–82 (2003).
- 484 24. Pereira, I. A. C. *et al.* A comparative genomic analysis of energy metabolism in sulfate  
485 reducing bacteria and archaea. *Front. Microbiol.* **2**, 69 (2011).
- 486 25. Santos, A. A. *et al.* A protein trisulfide couples dissimilatory sulfate reduction to energy  
487 conservation. *Science* **350**, 1541–1545 (2015).
- 488 26. Wagner, M., Roger, A. J., Flax, J. L., Brusseau, G. A. & Stahl, D. A. Phylogeny of  
489 dissimilatory sulfite reductases supports an early origin of sulfate respiration. *J. Bacteriol.*  
490 **180**, 2975–2982 (1998).
- 491 27. Müller, A. L., Kjeldsen, K. U., Rattei, T., Pester, M. & Loy, A. Phylogenetic and  
492 environmental diversity of DsrAB-type dissimilatory (bi)sulfite reductases. *ISME J.* **9**,  
493 1152–1165 (2015).
- 494 28. Meyer, B. & Kuever, J. Phylogeny of the alpha and beta subunits of the dissimilatory  
495 adenosine-5'-phosphosulfate (APS) reductase from sulfate-reducing prokaryotes - origin  
496 and evolution of the dissimilatory sulfate-reduction pathway. *Microbiology* **153**, 2026–  
497 2044 (2007).
- 498 29. Frolov, E. N. *et al.* Sulfate reduction and inorganic carbon assimilation in acidic thermal  
499 springs of the Kamchatka peninsula. *Microbiology* **85**, 471–480 (2016).
- 500 30. Prokofeva, M. I. *et al.* Cultivated anaerobic acidophilic/acidotolerant thermophiles from  
501 terrestrial and deep-sea hydrothermal habitats. *Extremophiles* **9**, 437–448 (2005).
- 502 31. Gumerov, V. M. *et al.* Complete genome sequence of *Vulcanisaeta moutnovskia* strain  
503 768-28, a novel member of the hyperthermophilic crenarchaeal genus *Vulcanisaeta*. *J.*  
504 *Bacteriol.* **193**, 2355–6 (2011).
- 505 32. Brüchert, V., Knoblauch, C. & Jorgensen, B. B. Controls on stable sulfur isotope  
506 fractionation during bacterial sulfate reduction in arctic sediments. *Geochim. Cosmochim.*  
507 *Acta* **65**, 763–776 (2001).
- 508 33. Meier, J., Piva, A. & Fortin, D. Enrichment of sulfate-reducing bacteria and resulting  
509 mineral formation in media mimicking pore water metal ion concentrations and pH  
510 conditions of acidic pit lakes. *FEMS Microbiol. Ecol.* **79**, 69–84 (2012).
- 511 34. Rinke, C. *et al.* Insights into the phylogeny and coding potential of microbial dark matter.  
512 *Nature* **499**, 431–437 (2013).
- 513 35. Huwiler, S. G. *et al.* One-megadalton metalloenzyme complex in *Geobacter*  
514 *metallireducens* involved in benzene ring reduction beyond the biological redox window.  
515 *Proc. Natl. Acad. Sci. U. S. A.* 201819636 (2019). doi:10.1073/pnas.1819636116
- 516 36. Colman, D. R. *et al.* Phylogenomic analysis of novel Diaforarchaea is consistent with  
517 sulfite but not sulfate reduction in volcanic environments on early Earth. *ISME J.* (2020).  
518 doi:10.1038/s41396-020-0611-9
- 519 37. Meyer, B. & Kuever, J. Molecular analysis of the distribution and phylogeny of  
520 dissimilatory adenosine-5'-phosphosulfate reductase-encoding genes (aprBA) among  
521 sulfur-oxidizing prokaryotes. *Microbiology* **153**, 3478–3498 (2007).
- 522 38. Watanabe, T., Kojima, H. & Fukui, M. Identity of major sulfur-cycle prokaryotes in  
523 freshwater lake ecosystems revealed by a comprehensive phylogenetic study of the  
524 dissimilatory adenylylsulfate reductase. *Sci. Rep.* **6**, 36262 (2016).
- 525 39. Ramos, A. R., Keller, K. L., Wall, J. D. & Cardoso Pereira, I. A. C. The membrane  
526 qmoABC complex interacts directly with the dissimilatory adenosine 5'-phosphosulfate

- 527 reductase in sulfate reducing bacteria. *Front. Microbiol.* **3**, 137 (2012).
- 528 40. Zane, G. M., Yen, H. C. & Wall, J. D. Effect of the deletion of *qmoABC* and the  
529 promoter-distal gene encoding a hypothetical protein on sulfate reduction in *Desulfovibrio*  
530 *vulgaris* Hildenborough. *Appl. Environ. Microbiol.* **76**, 5500–5509 (2010).
- 531 41. Buckel, W. & Thauer, R. K. Flavin-Based Electron Bifurcation, A New Mechanism of  
532 Biological Energy Coupling. *Chem. Rev.* **118**, 3862–3886 (2018).
- 533 42. Wagner, T., Koch, J., Ermler, U. & Shima, S. Methanogenic heterodisulfide reductase  
534 (HdrABC-MvhAGD) uses two noncubane [4Fe-4S] clusters for reduction. *Science* **357**,  
535 699–703 (2017).
- 536 43. Roychoudhury, A. N. Sulfate respiration in extreme environments: A kinetic study.  
537 *Geomicrobiol. J.* **21**, 33–43 (2004).
- 538 44. Pimenov, N. V. & Bonch-Osmolovskaya, E. A. 2 In Situ Activity Studies in Thermal  
539 Environments. *Methods Microbiol.* **35**, 29–53 (2006).
- 540 45. Chernyh, N. A. *et al.* Microbial life in Bourlyashchy, the hottest thermal pool of Uzon  
541 Caldera, Kamchatka. *Extremophiles* **19**, 1157–1171 (2015).
- 542 46. Dhillon, A., Goswami, S., Riley, M., Teske, A. & Sogin, M. Domain evolution and  
543 functional diversification of sulfite reductases. *Astrobiology* **5**, 18–29 (2005).
- 544 47. Sousa, F. L. *et al.* Early bioenergetic evolution. *Philos. Trans. R. Soc. Lond. B. Biol. Sci.*  
545 **368**, 20130088 (2013).
- 546

547

## 548 **ONLINE METHODS**

### 549 **Environmental sampling**

550 The sample used in this work was collected from Oreshek Spring (N52° 31.818 E158° 11.499, T  
551 91°C, pH 3.5) at the foot of Moutnovsky volcano (Kamchatka Peninsula, Russia). The sample of  
552 thermal water and sediment was placed into 50-mL glass vial with gas-tight butyl rubber stopper  
553 and aluminium screw cap, which was filled to capacity, hermetically sealed, and transported to  
554 the laboratory at ambient temperature. For DNA isolation, a mixed sample of sediment and water  
555 was used. Prior to arrival in the laboratory, the fixed sample was stored at ambient temperature  
556 for several days and then at –20°C until evaluation.

557

### 558 **Microbial cultures**

559 The following cultures were obtained from DSMZ: *Thermoproteus tenax* DSM2078<sup>T</sup>,  
560 *Vulcanisaeta souniana* DSM 14430<sup>T</sup>, *Vulcanisaeta distributa* DSM 14429<sup>T</sup>, and *Caldivirga*  
561 *maquilingensis* DSM 13496<sup>T</sup>. The purity and identity of the cultures were checked by 16S rRNA  
562 gene amplification and sequencing.

563 The binary culture 768-28 (referred to as “the binary culture”) containing “*Candidatus V.*  
564 *moutnovskia*” was initially regarded as a pure isolate<sup>30</sup>. The culture was obtained on medium  
565 with ethanol, yeast extract, and sulphate, but was then routinely maintained on medium with  
566 yeast extract and elemental sulphur, which provided for better growth. Later it was found that  
567 this culture contained an additional organism, besides the *Vulcanisaeta* sp., belonging to the

568 genus *Thermoproteus*. The genomes of both components were previously sequenced, closed and  
569 annotated<sup>31,48</sup>. The *Vulcanisaeta* component was found to represent a novel species named  
570 “*Candidatus* *Vulcanisaeta* *moutnovskia*” with 98% 16S rRNA gene similarity to *Vulcanisaeta*  
571 *distributa*<sup>20</sup>, while the *Thermoproteus* component had 100% 16S rRNA gene similarity with  
572 *Thermoproteus* *uzoniensis*<sup>49</sup>. For the present studies the binary culture<sup>30</sup> was obtained from M.I.  
573 Prokofeva (Federal Research Center of Biotechnology, RAS). The culture grows robustly on  
574 medium with yeast extract and sulphur or sulphate, and is maintained in sulphate conditions.  
575 Liquid medium of the following composition was used (g L<sup>-1</sup>): NH<sub>4</sub>Cl, 0.33; KCl, 0.33;  
576 MgCl<sub>2</sub>·2H<sub>2</sub>O, 0.33; CaCl<sub>2</sub>·6H<sub>2</sub>O, 0.33; KH<sub>2</sub>PO<sub>4</sub>, 0.33; Na<sub>2</sub>S·9H<sub>2</sub>O, 0.5; yeast extract, 1.0; trace  
577 element solution<sup>50</sup>, 1 ml; vitamin solution<sup>51</sup>. Sodium sulphide (0.5 g L<sup>-1</sup>) was used as a reducing  
578 agent. Resazurin (1.0 mg L<sup>-1</sup>) was added as a redox indicator. Na<sub>2</sub>SO<sub>4</sub> (1.0 g L<sup>-1</sup>) and S<sup>0</sup> (10.0 g  
579 L<sup>-1</sup>) were used as electron acceptors. To adjust the pH of the medium to 5.5 (for *T. tenax*), 4.8  
580 (for *V. souniana*, *V. distributa* and the binary culture) and 4.0 (for *C. maquilingensis*), 3N HCl  
581 was added. The medium was dispensed in 5-ml portions into 17-ml Hungate tubes; the  
582 headspace was filled with CO<sub>2</sub>. The incubation temperature was 85°C.  
583 Peptone (1 g L<sup>-1</sup>), glucose, lactose, maltose, sucrose (5 mM each), acetate, lactate, pyruvate,  
584 malate, propionate, butyrate, fumarate, succinate, citrate, ethanol, propanol, glycerol, methanol  
585 (20 mM each), glycine, leucine, tyrosine, serine, glutamate, glutamine, aspartate, asparagine,  
586 phenylalanine, alanine, lysine, arginine, histidine, cysteine, valine, proline, methionine (20 mM  
587 each), CO (N<sub>2</sub>/CO = 1:1, 4:1, or 20:1, v/v), and H<sub>2</sub> (H<sub>2</sub>/CO<sub>2</sub> = 80:20, v/v) were tested as  
588 alternative electron donors for the binary culture.

589

#### 590 **Radioisotopic tracing of sulphate reduction**

591 Sulphate reduction rates were measured by means of the radioisotope technique using <sup>35</sup>S-  
592 sulphate. Radioisotope experiments were performed in the laboratory using 15-mL Hungate  
593 tubes with screw caps. Each tube contained 5 mL of the medium. The headspace was filled with  
594 100% CO<sub>2</sub>, 10% inoculum was introduced, and 0.2 mL of <sup>35</sup>SO<sub>4</sub><sup>2-</sup> (37 × 10<sup>4</sup> Bq) was injected into  
595 each tube with a syringe through the stopper. The tubes were incubated in thermostats at a  
596 temperature of 85 °C for 4 days; after incubation, the samples were fixed with 1 mL of 2 M  
597 NaOH. The subsequent treatment was performed as described previously<sup>44</sup>.

598

#### 599 **DNA isolation**

600 Sediment samples (2-4 ml) were placed in centrifuge tubes and precipitated for 10 min at  
601 12,000×g and 4 °C. Sediment samples were resuspended in TNE buffer, pH 7.4 (20 mM Tris, 15  
602 mM NaCl, 20 mM EDTA), frozen in liquid nitrogen, ground, and melted in a water bath at 37°C.

603 The freezing and melting cycle was repeated twice. Lysozyme (200  $\mu\text{g ml}^{-1}$ ) and RNase (DNase-  
604 free, 5  $\mu\text{g ml}^{-1}$ ) were added, and the mixture was incubated for 30 min at room temperature.  
605 Proteinase K (5-10  $\mu\text{g ml}^{-1}$ ) and SDS (0.5%) were added, and the mixture was incubated for 30  
606 min at 54°C. After mixing, and cooling, an equal volume of a cooled phenol - chloroform -  
607 isoamyl alcohol (50:50:1) mixture was added, followed by agitation for 10 min and  
608 centrifugation for 10 min at 12,000 $\times$ g. The water phase was collected, supplemented with an  
609 equal volume of chloroform, agitated for 5 min, centrifuged, the water phase was collected, and  
610 chloroform extraction was repeated. 0.1 volume of 3 M sodium citrate (pH 5.2) and two volumes  
611 of cooled 96% ethanol were added to the water phase. For DNA precipitation, the mixture was  
612 allowed to stay at -20 °C for 60 min. DNA was gathered by centrifugation for 5 min at 12,000 $\times$ g,  
613 washed with 70 and 96% ethanol, dried, and dissolved in TE buffer (10 mM Tris, 1 mM EDTA,  
614 pH 7.4). 5  $\mu\text{l}$  of the preparation was applied to 1% agarose gel for the DNA visualisation.

615

#### 616 **PCR, DGGE, and qPCR analyses**

617 The following primers were used in this work for amplification of 16S rRNA genes of Bacteria  
618 and Archaea: Bact338F- ACTCCTACGGGAGGCAGCAG<sup>52</sup> and Bact907R-  
619 CCGTCAATTCMTTGTGAGTTT<sup>53</sup> and A338F- GGCCCTAYGGGGYGCASCAGGC<sup>54</sup> and  
620 A915R- GTGCTCCCCCGCCAATTCCT<sup>55</sup>. 20  $\mu\text{l}$  of the PCR mixture contained 2  $\mu\text{l}$  of 10 $\times$   
621 buffer (Eurogen buffer with 1.5 mM  $\text{MgCl}_2$ ); deoxynucleoside triphosphates (Eurogen, Russia),  
622 200  $\mu\text{M}$  each; 20 pmol of each of the Bact338F and Bact907R or A338F and A915R primers; 1.2  
623 U of *Taq* polymerase (Eurogen); and approximately 10 ng of DNA. The PCR mixture was  
624 incubated for 5 min at 94°C, followed by 33 cycles of 30 s at 93°C, 30 s at 52°C (bacterial  
625 primer system) or 68°C (archaeal primer system), and 60 sec at 72°C, with final extension at  
626 72°C for 10 min.

627 The following primers were used for amplification of *dsrAB* genes of “*Candidatus V.*  
628 *moutnovskia*”: N1 Vmut592F 5’AAAATAAAGTTCAAGTTTGTGGTTGTCCAATGG and  
629 N2 Vmut 2021R 5’- TATGCACTTCTCTCATCAACCTCAATACC. The PCR mixture was  
630 incubated for 5 min at 94°C, followed by 33 cycles of 30 s at 93°C, 30 s at 69°C, and 120 sec at  
631 72°C, with final extension at 72°C for 20 min.

632

633

#### 634 **High-throughput sequencing of 16S rRNA gene fragments**

635 The V4 region of 16S rRNA genes was amplified, and libraries were prepared as described by  
636 Caporaso et al.<sup>56</sup>, with some modification. The following primer set was used for amplification:  
637 the forward primer was 5’-AATGATACGGCGACCACCGAGATCTACAC TATGGTAATT

638 GTGTGBCAGCMGCCGCGGTAA-3', consisting of 5' Illumina adapter, forward primer pad,  
639 forward primer linker and 515f primer<sup>57</sup> and the reverse primer was 5'-  
640 CAAGCAGAAGACGGCATAACGAGAT XXXXXXXXXXXXX AGTCAGTCAG CC  
641 GGACTACHVGGGTATCTAAT-3', consisting of reverse complement of 3' Illumina adapter,  
642 Golay barcode, reverse primer pad, reverse primer linker and 806R primer<sup>56</sup>. Each sample was  
643 amplified in two replicates, which were then pooled into a single volume and run on a standard  
644 agarose gel for visualisation and size selection purposes. Prior to sequencing, equal amounts of  
645 amplicon DNA from each sample were combined to create a single library pool, which was then  
646 diluted to a concentration of 4 nM according to the Illumina Sample Preparation Guide. Library  
647 denaturation and sample loading were performed according to the Illumina Sample Preparation  
648 Guide using a MiSeq Reagent Kit v3 (600 cycles) (Illumina). The sequencing of the library was  
649 performed with the Illumina MiSeq platform. Most of the data analysis, including quality  
650 trimming, demultiplexing, taxonomic assignments, and core diversity analyses were performed  
651 with QIIME (version 1.9.1<sup>62</sup>) and SILVA online data analysis service<sup>58</sup>. The coverage of the  
652 microbial community was estimated by determining Chao1 richness<sup>59</sup>.

653

#### 654 **Analytical methods**

655 Sulphide formation was determined using the colourimetric method with N,N-dimethyl-para-  
656 phenylenediamine<sup>60</sup>; the developing blue colouration was quantified by spectrophotometry at  $\lambda =$   
657 670 nm. Sulphate ion concentrations were determined on a Stayer ion chromatograph (Russia).

658

#### 659 **Proteomics**

660 Proteomic analysis of the binary sulphate-reducing archaeal culture 768-28, grown with sulphate  
661 and with sulphur as electron acceptors (see above), was performed by liquid chromatography and  
662 mass spectrometry analysis. In order to guarantee access to the highest diversity and amount of  
663 proteins two different methods for protein extraction were used. First, one (Method I)<sup>61</sup> involving  
664 extraction with a multi-chaotropic lysis buffer containing a non-denaturing zwitterionic  
665 detergent, most efficient for extracting cytosolic proteins. Second, one (Method II) involving a  
666 denaturing anionic detergent allowing total disruption of the membranes and capable of  
667 extracting both membrane (hydrophobic) and non-membrane (water-soluble, hydrophilic)  
668 proteins. Following extraction, 1D-nano Liquid Chromatography Electrospray Ionization  
669 Tandem Mass Spectrometric (LC ESI-MSMS) analysis with Triple TOF 5600 and Orbitrap  
670 technologies were used for protein identification. Extensive description of methods for protein  
671 extraction based on a non-denaturing detergent and on a denaturing detergent, protein digestion,

672 and liquid chromatography and mass spectrometry analysis are provided was performed as  
673 described previously<sup>61</sup>.

674

675 *Proteomic analyses based on denaturing detergent (Method II)*

676 *Lysis and protein extraction.* Cell pellets were dissolved with multi-chaotropic lysis buffer  
677 containing 7 M urea (USB Corporation, Cleveland, OH), 2 M thiourea (Sigma-Aldrich), 5 %  
678 SDS (Sigma-Aldrich), 100 mM triethylammonium bicarbonate (TEAB) (Thermo Fisher  
679 Scientific) and a protease/phosphatase inhibitor cocktail (Thermo Fisher Scientific). Samples  
680 were reduced and alkylated by adding 5 mM tris(2-carboxyethyl)phosphine and 10 mM  
681 chloroacetamide for 1 hour at 37°C and homogenized by micro tip probe ultrasonication for 1  
682 min on UP50H ultrasonic lab homogenizer (Hielscher Ultrasonics). The homogenate was  
683 centrifuged at 16,000 × g for 15 min at 4°C, and the supernatant containing the solubilized  
684 proteins was used for further analysis. Protein concentration was estimated by Pierce 660nm  
685 protein assay (Thermo Fisher Scientific).

686

687 *S-Trap<sup>TM</sup> Digestion.* Protein digestion in the S-Trap filter (Protifi, Huntington, NY, USA) was  
688 performed following the manufacturer's procedure with slight modifications. Briefly, 20 µg of  
689 protein of each sample was diluted to 40 µL with 5% SDS. Afterwards, 12% phosphoric acid and  
690 then seven volumes of binding buffer (90% methanol; 100 mM TEAB) were added to the sample  
691 (final phosphoric acid concentration: 1.2%). After mixing, the protein solution was loaded to an  
692 S-Trap filter in two consecutive steps, separated by a 2 min centrifugation at 3,000×g. Then the  
693 filter was washed 3 times with 150 µL of binding buffer. Finally, 1 µg of Pierce MS-grade  
694 trypsin (Thermo-Fisher Scientific) in 20 µL of a 100 mM TEAB solution was added to each  
695 sample in a ratio 1:20 (w/w) and spun through the S-Trap prior to digestion. Flow-through was  
696 then reloaded to the top of the S-Trap column and allowed to digest in a wet chamber at 37°C  
697 overnight. To avoid liquid leakage from the S-Trap column, a customized yellow tip with 9  
698 Empore 3M C18 disks (Sigma-Aldrich) was placed at the bottom tip of the S-Trap column  
699 during digestion. To elute peptides, two step-wise buffers were applied (1) 40 µL of 25 mM  
700 TEAB and 2) 40 µL of 80% acetonitrile and 0.2% formic acid in H<sub>2</sub>O), separated by a 2 min  
701 centrifugation at 3,000×g in each case. Eluted peptides were pooled and vacuum centrifuged to  
702 dryness.

703

704 MS/MS data obtained for individual samples were processed using Analyst® TF 1.7 Software  
705 (SCIEX) (for Method I) and Proteome Discoverer v2.4 (Thermo Fisher Scientific) (for Method  
706 II). Raw data file conversion tools generated mgf files which were also searched against protein

707 database that included “*Candidatus V. moutnovskia*” and *Thermoproteus uzoniensis* protein  
708 sequences from Uniprot/Swissprot Knowledgebase (last update: 2020/03/04, 4.573 sequences)  
709 using the Mascot Server v. 2.5.1 (Matrix Science, London, UK) (for Method I) or Mascot Server  
710 v2.7.0.1 (Matrix Science, London, UK) (for Method II). Search parameters were set as follows:  
711 enzyme, trypsin; allowed missed cleavages, 2; carbamidomethyl (C) as fixed modification and  
712 acetyl (Protein N-term), Gln to pyro-Glu (N-term Q), Glu to pyro-Glu (N-term E) and Oxidation  
713 (M) as variable modifications. Peptide mass tolerance was set to 25 ppm and 0.05 Da for  
714 fragment masses derived from Method I and  $\pm 10$  ppm for precursors and 0.02 Da for fragment  
715 masses from Method II. The confidence interval for protein identification was set to  $\geq 95\%$   
716 ( $p < 0.05$ ) and only peptides with an individual ion score above the 1% False Discovery Rates  
717 (FDR) at spectra level were considered correctly identified. The threshold of only one identified  
718 peptide per protein identification was used because FDR controlled experiments counter-  
719 intuitively suffer from the two-peptide rule<sup>61</sup>.

720 To rank the protein abundance in each sample, the Exponentially Modified Protein  
721 Abundance Index (emPAI) was used in the present study as a relative quantitation score of the  
722 proteins in a complex mixture based on protein coverage by the peptide matches in a database  
723 search result<sup>62</sup>.

724

## 725 **Genomic analysis**

726 The genome analyses of “*Candidatus V. moutnovskia*” and other archaea were performed at the  
727 site <https://blast.ncbi.nlm.nih.gov/Blast.cgi>. Protein sequences of known sulphate reducing  
728 organisms were used as queries for blastp: *Desulfovibrio vulgaris ssp. vulgaris* str.  
729 Hildenborough (Sat – AAS95773, AprA – AAS95326, AprB – AAS95327, DsrA – AAS94885,  
730 DsrB – AAS94886, DsrC – AAS97248, DsrJ – AAS95766, DsrK – AAS95767, DsrM –  
731 AAS95768, DsrO – AAS95765, DsrP – AAS95764, HdrA – AAS96875, HdrB – AAS96876,  
732 HdrC – AAS96877, PpaC – AAS96114, QmoA – AAS95328, QmoB – AAS95329, QmoC –  
733 AAS95330), and *Archaeoglobus fulgidus* DSM 4304 (Sat – AAB89581, AprA – AAB89579,  
734 AprB – AAB89580, DsrA – AAB90812, DsrB – AAB90811, DsrC – AAB89026, DsrJ –  
735 AAB90740, DsrK – AAB90735, DsrM – AAB90736, DsrO – AAB90738, DsrP – AAB90737,  
736 HdrA – AAB89867, HdrB – AAB89869, HdrC – AAB89868, PpaC – AAB90480, QmoA –  
737 AAB90578, QmoB – AAB90579, QmoC – AAB90580). In addition, *Caldivirga maquilingensis*  
738 IC-167 (HppA – ABW01781), *Syntrophobacter fumaroxidans* MPOB (HppA – ABK18711),  
739 *Allochromatium vinosum* DSM 180 (AprM – ADC62058) and *Hyphomicrobium denitrificans*  
740 (HdrA – WP\_013214728.1) were used as queries. The locus tags of the “*Candidatus V.*

741 moutnovskia" sulphate reduction genes and their function are described in Supplementary Figure  
742 1.

743

#### 744 **Phylogenetic analysis**

745 A dataset consisting of 289 archaeal genomes (253 complete and 36 assembled as contigs or  
746 scaffolds) and 4,856 complete bacterial genomes were downloaded from NCBI and JGI  
747 (Supplementary Table S4) and mapped to NCBI taxonomy. The completeness and contamination  
748 of metagenomic records were retrieved from the original publication. Proteins involved in  
749 sulphate reduction were identified using the reciprocal best BLAST hit (rBBH) approach  
750 (version 2.4.0+)<sup>63</sup> ( $E$ -value  $\leq 10^{-10}$  and identity cut-off of 25%) using as queries proteins from  
751 characterised bacterial and archaeal sulphate reducers (see Genomic analysis). Pairwise-global  
752 identities were calculated considering local identity, sequence and alignment length. Recent  
753 duplications, defined as sequences with identity  $\geq 70\%$  to identified rBBHs, were kept. Hits were  
754 mapped using NCBI feature tables and gene clusters were plotted using in-house Perl scripts, R-  
755 Studio (version 1.0.153) and R-package genoPloR<sup>64</sup> (version 0.1). The syntheny allowed the  
756 identification of canonical sequences of *hdrAs* from several methanogens and sulphate reducers  
757 organised in an *hdrABC* cluster and the identification of (frameshifted) genes filtered out by  
758 coverage. Transmembrane (TM) helices prediction was performed with TMHMM (TMHMM  
759 Server v. 2.0)<sup>65</sup> using default parameters.

760 For phylogenetic analysis, the HdrA-like sequences from the metagenomic dataset were  
761 combined with the ones retrieved from the NCBI nr search. For the small *sat*, *aprA* and *aprB*  
762 phylogenies, 10 selected bacterial genomes of representative sulphate reducers and/or sulphur  
763 oxidisers from different phylogenetic lineages and 26 archaeal genomes from genera in which at  
764 least one genome contains *dsrAB* genes were considered. All alignments were performed with  
765 clustalw2<sup>66</sup> (version 2.1) and trimmed in TrimAl<sup>67</sup>. Furthermore, in the HdrA-like reconstruction,  
766 only the "HdrA domain" common to QmoA, QmoB and HdrA families and defined by the  
767 Conserved Domain Database at NCBI (CDD version 3.16 or higher) was considered. Maximum  
768 likelihood phylogenies were reconstructed using IQ-TREE<sup>68</sup> (version 1.5.2 or higher) with best  
769 model selection using 100 non-parametric bootstraps for the small reconstructions and 1,000  
770 ultrafast bootstraps for the large HdrA-like and AprA families. Phylogenies were rooted with the  
771 Minimal Ancestor Deviation method<sup>69</sup> and/or using succinate dehydrogenase/fumarate  
772 reductases as outgroup (*aprA*) and visualised in FigTree (version 1.4.3)  
773 (<http://tree.bio.ed.ac.uk/publications/>). Both *aprA* rooting methods selected the same root.

774 A combined analysis of sequence similarity, cofactor composition and syntheny, was  
775 used for the distinction between bona-fide *qmoA/B* genes and closely-related heterodisulphide

776 reductase genes (*hdr*), usually present in several copies with varied domain composition and  
777 functional role<sup>24,70</sup> in sulphur metabolising organisms.

778

- 779 48. Mardanov, A. V. *et al.* Complete genome sequence of the thermoacidophilic crenarchaeon  
780 *Thermoproteus uzoniensis* 768-20. *J. Bacteriol.* **193**, 3156–3157 (2011).
- 781 49. Bonch-Osmolovskaya, E. A., Miroshnichenko, M. L., Kostrikina, N. A., Chernych, N. A.  
782 & Zavarzin, G. A. *Thermoproteus uzoniensis* sp. nov., a new extremely thermophilic  
783 archaeobacterium from Kamchatka continental hot springs. *Arch. Microbiol.* **154**, 556–559  
784 (1990).
- 785 50. Wolin, E. A., Wolin, M. J. & Wolfe, R. S. Formation of methane by bacterial extracts. *J.*  
786 *Biol. Chem.* **238**, 2882–6 (1963).
- 787 51. Kevbrin, V. V., Zavarzin, G. A. Effect of Sulfur Compounds on the Growth of the  
788 Halophilic Homoacetic Bacterium *Acetohalobium arabaticum*. in *Microbiology -AIBS-*  
789 *C/C of Mikrobiologiia* 563 (Plenum Publishing Corporation, 1992).
- 790 52. Lane, D. J. 16S/23S rRNA Sequencing. in *Nucleic Acid Techniques in Bacterial*  
791 *Systematic* (ed. Stackebrandt, E. and Goodfellow, M.) 115–175 (John Wiley and Sons,  
792 1991).
- 793 53. Muyzer, G. & Smalla, K. Application of denaturing gradient gel electrophoresis (DGGE)  
794 and temperature gradient gel electrophoresis (TGGE) in microbial ecology. in *Antonie van*  
795 *Leeuwenhoek* 127–141 (1998). doi:10.1023/A:1000669317571
- 796 54. Kublanov, I. V. *et al.* Biodiversity of thermophilic prokaryotes with hydrolytic activities  
797 in hot springs of uzon caldera, kamchatka (Russia). *Appl. Environ. Microbiol.* **75**, 286–  
798 291 (2009).
- 799 55. Stahl, D.A. and Amann, R. Development and Application of Nucleic Acid Probes in  
800 Bacterial Systematics. in *Nucleic Acid Techniques in Bacterial Systematics* (ed.  
801 Stackebrandt, E. and Goodfellow, M.) 205–248 (John Wiley & Sons, Ltd, 1991).
- 802 56. Caporaso, J. G. *et al.* Global patterns of 16S rRNA diversity at a depth of millions of  
803 sequences per sample. *Proc. Natl. Acad. Sci. U. S. A.* **108**, 4516–4522 (2011).
- 804 57. Hugerth, L. W. *et al.* DegePrime, a program for degenerate primer design for broad-  
805 taxonomic-range PCR in microbial ecology studies. *Appl. Environ. Microbiol.* **80**, 5116–  
806 5123 (2014).
- 807 58. Quast, C. *et al.* The SILVA ribosomal RNA gene database project: improved data  
808 processing and web-based tools. *Nucleic Acids Res.* **41**, D590–D596 (2012).
- 809 59. Chao, A. Non-parametric estimation of the classes in a population. *Scand. J. Stat.* **11**,  
810 265–270 (1984).
- 811 60. Trueper, H. G. & Schlegel, H. G. Sulphur metabolism in Thiorhodoceae. I. Quantitative  
812 measurements on growing cells of *Chromatium okenii*. *Antonie Van Leeuwenhoek* **30**,  
813 225–38 (1964).
- 814 61. Sorokin, Di. Y. *et al.* Discovery of extremely halophilic, methyl-reducing euryarchaea  
815 provides insights into the evolutionary origin of methanogenesis. *Nat. Microbiol.* **2**, 1–11  
816 (2017).
- 817 62. Arike, L. & Peil, L. Spectral Counting Label-Free Proteomics. in *Methods in Molecular*  
818 *Biology* (ed. Martins-de-Souza, D.) 213–222 (Media, Springer Science + Business, 2014).
- 819 63. Altschul, S. F. *et al.* Gapped BLAST and PSI-BLAST: A new generation of protein  
820 database search programs. *Nucleic Acids Res.* **25**, 3389–3402 (1997).
- 821 64. Guy, L., Roat Kultima, J. & Andersson, S. G. E. genoPlotR: comparative gene and  
822 genome visualization in R. *Bioinformatics* **26**, 2334–2335 (2010).
- 823 65. Krogh, a, Larsson, B., von Heijne, G. & Sonnhammer, E. L. Predicting transmembrane  
824 protein topology with a hidden Markov model: application to complete genomes. *J. Mol.*  
825 *Biol.* **305**, 567–580 (2001).
- 826 66. Larkin, M. A. *et al.* Clustal W and Clustal X version 2.0. *Bioinformatics* **23**, 2947–2948

- 827 (2007).
- 828 67. Capella-Gutiérrez, S., Silla-Martínez, J. M. & Gabaldón, T. trimAl: A tool for automated  
829 alignment trimming in large-scale phylogenetic analyses. *Bioinformatics* **25**, 1972–1973  
830 (2009).
- 831 68. Nguyen, L.-T., Schmidt, H. A., von Haeseler, A. & Minh, B. Q. IQ-TREE: A Fast and  
832 Effective Stochastic Algorithm for Estimating Maximum-Likelihood Phylogenies. *Mol.*  
833 *Biol. Evol.* **32**, 268–274 (2015).
- 834 69. Tria, F. D. K., Landan, G. & Dagan, T. Phylogenetic rooting using minimal ancestor  
835 deviation. *Nat. Ecol. Evol.* **1**, 0193 (2017).
- 836 70. Grein, F., Ramos, A. R., Venceslau, S. S. & Pereira, I. A. C. Unifying concepts in  
837 anaerobic respiration: Insights from dissimilatory sulfur metabolism. *Biochim. Biophys.*  
838 *Acta - Bioenerg.* **1827**, (2013).
- 839 71. Perez-Riverol, Y. *et al.* The PRIDE database and related tools and resources in 2019:  
840 Improving support for quantification data. *Nucleic Acids Res.* **47**, D442–D450 (2019).
- 841

842

### 843 **Reporting summary**

844 Further information on research design is available in Reporting Summary linked to this article.

845

### 846 **Code availability**

847 The small scripts used in this paper are available at <https://figshare.com/s/fb5a1541be68639f4026>

848

### 849 **Data availability statement**

850 *Candidatus* *Vulcanisaeta mountnovskia* 768-28 has been deposited into the All-Russian  
851 Collection of Microorganisms (VKM) under the number VKM B-3479. The mass spectrometry  
852 proteomics data have been deposited in the ProteomeXchange Consortium via the PRIDE<sup>71</sup>  
853 partner repository with the dataset identifier PXD012750 and 10.6019/PXD012750.  
854 Pyrosequencing read data obtained for the 16S rRNA gene fragments were deposited in  
855 Sequence Read Archive (SRA) under the accession numbers [PRJNA642261](https://www.ncbi.nlm.nih.gov/PRJNA642261). To reproduce the  
856 results reported, the raw data are to be downloaded from SRA and submitted to the SILVAngs  
857 analysis platform (<https://ngs.arb-silva.de/silvangs/>). We did not obtain any new genomic  
858 assemblies, as the genomes used for computational analyses have already been reconstructed in  
859 previous and published work and are publicly available. The accession codes and taxonomic  
860 information of the genomes from the dataset are given in Supplementary Table S4. The binary  
861 culture genomes used here have been previously sequenced and published<sup>31,48</sup> and have the  
862 accession codes (GenBank CP002529, CP002590). The alignments and phylogenies at the basis  
863 of Figures 3, and 5 and Extended Data Figures 8, 9 and 10 are available in Figshare  
864 (<https://figshare.com/s/fb5a1541be68639f4026>). The source data for Figures 1, and 2 and  
865 Extended Data Figures 2, 3, 4, 5, 6, and 7 are given in this paper and in its supplementary  
866 information.

867

868

869 **Correspondence and requests for materials** should be addressed to NAC, FLS and IAC.

870

## 871 **ACKNOWLEDGMENTS**

872 We thank Giddy Landan for sharing with us the updated version of the minimal ancestor  
873 deviation method. This work was supported in part by grant # 1774-30025 of the Russian  
874 Science Foundation, Program “Molecular and Cell Biology” of the Russian Academy of  
875 Sciences, as well as grant # 13-04-01695 of the Russian Foundation for Basic Research and grant  
876 of the Ministry of Science and Higher Education of the Russian Federation (to N.A.C., A.V.L.,  
877 E.N.F., M.L.M., A.Y.M., N.V.P. and E.A.B-O). Sequencing of PCR amplicons was performed  
878 using the scientific equipment of the Core research facility “Bioengineering” by Tatyana  
879 Kolganova. The proteomic analysis was performed in the Proteomics Facility of The Spanish  
880 National Center for Biotechnology (CNB-CSIC), which belongs to ProteoRed, PRB2-ISCIII,  
881 supported by grant PT13/0001 (to S.C., M.C.M., M.F.). P.N.G. acknowledges the funding of the  
882 UK Biotechnology and Biological Sciences Research Council (BBSRC) within the ERA NET-  
883 IB2 program, grant number ERA-IB-14-030 and European Union Horizon 2020 research and  
884 innovation program [Blue Growth: Unlocking the potential of Seas and Oceans] under grant  
885 agreement No [634486] and the support of the Centre of Environmental Biotechnology (CEB)  
886 Project part-funded by the European Regional Development Fund (ERDF) through the Welsh  
887 Government and the support of the Centre of Environmental Biotechnology (CEB). D.Y.S. was  
888 supported by the SIAM/Gravitation Program (Dutch Ministry of Education and Science, grant  
889 24002002) and RFBR grant 19-04-00401. F.L.S. and S.N. acknowledge support from the Wiener  
890 Wissenschafts, Forschungs- und Technologiefonds (Austria) through the grant VRG15-007.  
891 F.L.S. gratefully acknowledges funding from the European Research Council (ERC) under the  
892 European Union’s Horizon 2020 research and innovation programme (grant agreement 803768).  
893 I.A.C.P. acknowledges support from the Fundação para a Ciência e Tecnologia (Portugal)  
894 through grant PTDC/BIA-BQM/29118/2017 and R&D unit MOSTMICRO-ITQB  
895 (UIDB/04612/2020 and UIDP/04612/2020).

896

## 897 **Author contributions**

898 N.A.C. designed the research. N.A.C. and E.N.F. performed the fieldwork and sediment activity  
899 determinations. E.N.F. and M.L.M. enriched and isolated pure cultures and performed their  
900 microbiological studies. S.N., F.L.S., N.A.C. and A.V.L. performed genomic analysis and  
901 evolutionary reconstructions. A.Y.M. analysed 16S rRNA genes in sediments and carried out

902 qPCR. N.V.P. performed radioisotope research. S.C., M.C.M., M.F. and P.N.G. performed  
903 proteomic analysis. N.A.C., A.V.L., I.A.C.P., F.L.S, S.N., E.N.F., D.Y.S. and E.A.B-O analysed  
904 the data and wrote the paper. All authors have seen and approved the final version submitted.

905

906 **Competing interests**

907 All local, national and international regulations and conventions, and normal scientific ethical  
908 practices have been respected. The authors state no conflicts of interest.

909

910

911

912 **Figure Legends**

913

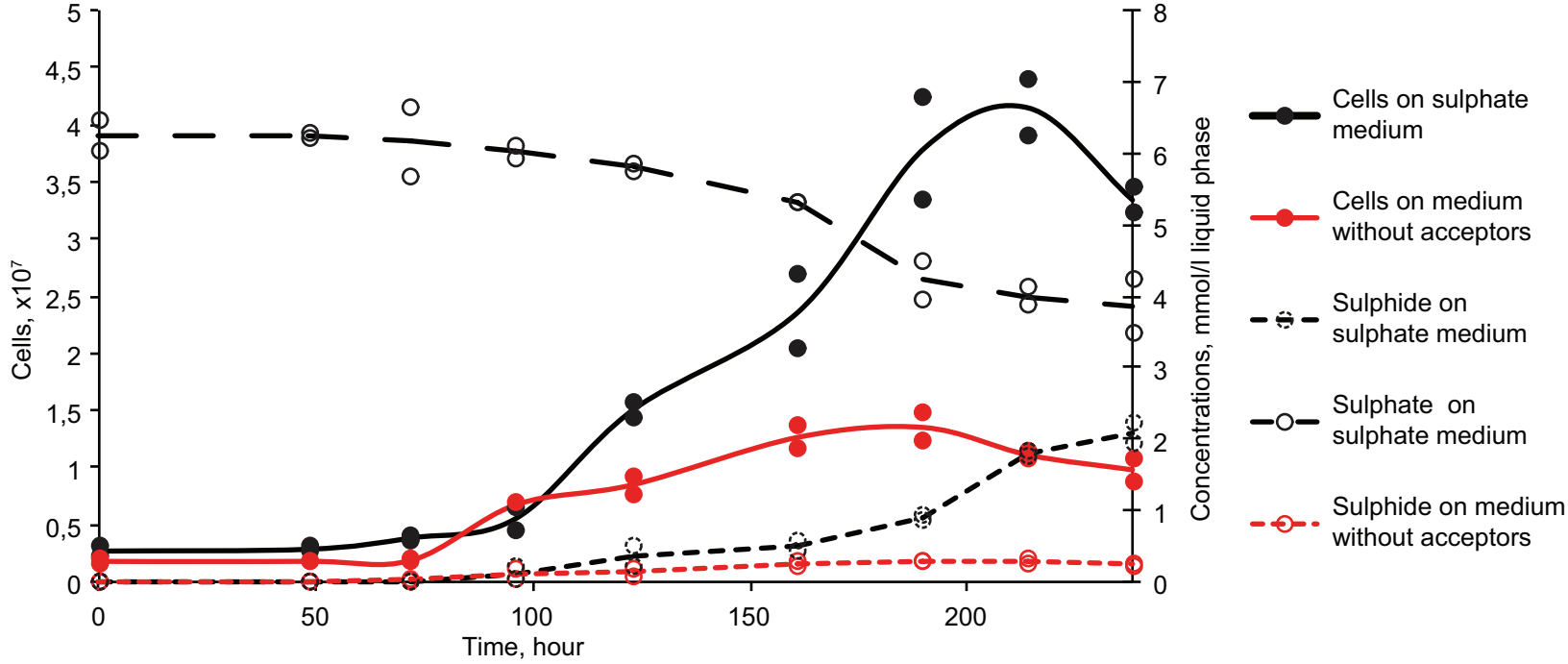
914 **Fig. 1. Growth of the binary culture on sulphate.** Data points shown correspond to 2  
915 independent growth experiments. Lines represent the mean of  $n = 2$  independent experiments.

916 **Fig. 2. Distribution of sulphate reduction/sulphur oxidation genes in archaea versus**  
917 **established bacterial groups.** Only organisms belonging to genera in which *dsr* genes are found  
918 are represented in the figure. When experimentally known, the initial substrate of the enzyme set  
919 is indicated in the first column. Abbreviations: HppA/ PpaC, pyrophosphatases, Sat, sulphate  
920 adenylyl transferase; AprAB, APS reductase; DsrABCKM, genes involved in dissimilatory  
921 sulphite reduction/oxidation; Qmo complex, QmoABC; in some sulphur oxidisers AprM,  
922 instead of QmoABC, is the physiological partner of AprAB, providing a link to the membrane.

923 **Fig. 3. Phylogenetic analysis of AprA proteins.** Maximum likelihood reconstruction  
924 (LG+I+G4) of AprA and AprA-like proteins. The tree was rooted by using as outgroup succinate  
925 dehydrogenases. The same root was obtained by the minimal ancestor deviation method<sup>73</sup>. Black  
926 circles indicate support values of 100, and all other node support values are omitted for  
927 simplicity. The scale bar indicates number of substitutions per site.

928 **Fig. 4. Gene synteny and cofactor composition of the QmoAB/HdrA family.**

929 **Fig. 5. Phylogenetic analysis of HdrA-like proteins, including QmoA and QmoB.** Maximum-  
930 likelihood reconstruction (LG+I+G4) of the HdrA-domain showing the expanded “*Candidatus*  
931 *V. moutnovskia*” QmoA (a) and QmoB (b) clades. The full tree is given in Extended Data Figure  
932 10. The scale bar indicates number of substitutions per site.



	substrate	HppA/ PpaC	Sat	AprA	AprB	DsrA	DsrB	DsrC	DsrM	DsrK	QmoA	QmoB	QmoC	AprM
<b>Thermoproteaceae</b>														
<i>Candidatus V. moutnovskia</i> 768-28	SO <sub>2</sub> <sup>-2</sup>	●	●	●	●	●	●	●	●	●	●	●	●	
<i>Vulcanisaeta distributa</i> DSM 14429	SO <sub>3</sub> <sup>-2</sup>	●	●	●	●	●	●	●	●	●	●	●	●	
<i>Vulcanisaeta souniana</i> JCM 11219	SO <sub>3</sub> <sup>-2</sup>	◐	◐	◐	●	●	●	●	●	●	◐	◐	◐	
<i>Caldivirga maquilingensis</i> IC-167	SO <sub>3</sub> <sup>-2</sup>	●	●	●	●	●	●	●	●	●	●	●	●	
<i>Caldivirga</i> sp. MU80*	SO <sub>3</sub> <sup>-2</sup>	●	●	●	●	●	●	●	●	●	○	○	◐	
<i>Caldivirga</i> sp. Obs2 genome 27**	SO <sub>4</sub> <sup>-2</sup>	●	●	◐	●	●	●	●	●	●	●	●	●	
<i>Thermoproteus uzoniensis</i> 768-20	sulfur	●	●	●	●	●	●	●	●	●	●	●	●	
<i>Thermoproteus tenax</i> Kra 1	SO <sub>3</sub> <sup>-2</sup>	●	●	●	●	●	●	●	●	●	●	●	●	
<i>Pyrobaculum ferrireducens</i>	SO <sub>3</sub> <sup>-2</sup>	●	●	●	●	●	●	●	●	●	●	●	●	
<i>Pyrobaculum oguniense</i> TE7	SO <sub>3</sub> <sup>-2</sup>	●	●	●	●	●	●	●	●	●	●	●	●	
<i>Pyrobaculum calidifontis</i> JCM 11548	SO <sub>3</sub> <sup>-2</sup>	●	●	●	●	●	●	●	●	●	●	●	●	
<i>Pyrobaculum arsenaticum</i> DSM 13514	SO <sub>3</sub> <sup>-2</sup>	●	●	●	●	●	●	●	●	●	●	●	●	
<i>Pyrobaculum islandicum</i> DSM 4184	SO <sub>3</sub> <sup>-2</sup>	●	●	●	●	●	●	●	●	●	●	●	●	
<i>Pyrobaculum neutrophilum</i> V24Sta	SO <sub>3</sub> <sup>-2</sup>	●	●	●	●	●	●	●	●	●	●	●	●	
<i>Pyrobaculum aerophilum</i> str. IM2	thiosulfate	●	●	◐	◐	●	●	●	●	●	●	●	●	
<b>Korarchaeota</b>														
<i>Ca. Korarchaeum cryptofilum</i> OPF8	SO <sub>3</sub> <sup>-2</sup>	●	●	●	●	●	●	●	●	●	○	○	○	
<i>Ca. Methanodesulfokores washburnensis</i> MDKW*	SO <sub>3</sub> <sup>-2</sup>	●	●	●	●	●	●	●	●	●	○	○	○	
<i>Ca. Korarchaeum cryptofilum</i> WS*	SO <sub>3</sub> <sup>-2</sup>	●	●	●	●	●	●	●	●	●	○	○	○	
<b>Aigarchaeota</b>														
Unclassified Aigarchaeota JZ bin 15*	SO <sub>3</sub> <sup>-2</sup>	●	●	●	●	●	●	●	●	●	○	○	○	
<b>Hydrothermarchaeota</b>														
<i>Ca. Hydrothermarchaeota archaea</i> JdFR-18*	SO <sub>3</sub> <sup>-2</sup>	●	●	◐	◐	●	●	●	●	●	●	●	●	
<i>Ca. Hydrothermarchaeota archaea</i> JdFR-17**	SO <sub>3</sub> <sup>-2</sup>	●	●	◐	◐	●	●	●	●	●	●	●	●	
<i>Ca. Hydrothermarchaeota archaea</i> JdFR-16**	SO <sub>3</sub> <sup>-2</sup>	●	●	◐	◐	●	●	●	●	●	●	●	●	
<b>Archaeoglobus</b>														
<i>Archaeoglobus veneficus</i> SNP6	SO <sub>2</sub> <sup>-2</sup>	●	●	●	●	●	●	●	●	●	●	●	●	
<i>Archaeoglobus profundus</i> DSM 5631	SO <sub>4</sub> <sup>-2</sup>	●	●	●	●	●	●	●	●	●	●	●	●	
<i>Archaeoglobus sulfatcallidus</i> PM70-1	SO <sub>4</sub> <sup>-2</sup>	●	●	●	●	●	●	●	●	●	●	●	●	
<i>Archaeoglobus fulgidus</i> DSM 4304	SO <sub>2</sub> <sup>-2</sup>	●	●	●	●	●	●	●	●	●	●	●	●	
<i>Archaeoglobus fulgidus</i> DSM 8774	SO <sub>4</sub> <sup>-2</sup>	●	●	●	●	●	●	●	●	●	●	●	●	
<b>Bacterial dissimilatory sulfate reducers</b>														
<i>Desulfotomaculum reducens</i> MI-1	SO <sub>2</sub> <sup>-2</sup>	●	●	●	●	●	●	●	●	●	●	●	●	
<i>Ammonifex degensii</i> KC4	SO <sub>4</sub> <sup>-2</sup>	●	●	●	●	●	●	●	●	●	●	●	●	
<i>Thermodesulfobacterium geofontis</i> OPF15	SO <sub>4</sub> <sup>-2</sup>	●	●	●	●	●	●	●	●	●	●	●	●	
<i>Thermodesulfovibrio yellowstoni</i> DSM 11347	SO <sub>2</sub> <sup>-2</sup>	●	●	●	●	●	●	●	●	●	●	●	●	
<i>Desulfovibrio vulgaris</i> str. Hildenborough	SO <sub>4</sub> <sup>-2</sup>	●	●	●	●	●	●	●	●	●	●	●	●	
<b>Bacterial dissimilatory sulfur oxidizers</b>														
<i>Chlorobium phaeobacteroides</i> BS1	H <sub>2</sub> S	●	●	●	●	●	●	●	●	●	●	●	●	
<i>Chlorobium tepidum</i> TLS	H <sub>2</sub> S	●	●	●	●	●	●	●	●	●	●	●	●	
<i>Magnetospira</i> sp. QH-2	H <sub>2</sub> S	●	●	●	●	●	●	●	●	●	●	●	●	●
<i>Allochromatium vinosum</i> DSM 180	H <sub>2</sub> S	●	●	●	●	●	●	●	●	●	●	●	●	●
<i>Thiobacillus denitrificans</i> ATCC 25259	H <sub>2</sub> S	●	●	●	●	●	●	●	●	●	●	●	●	●

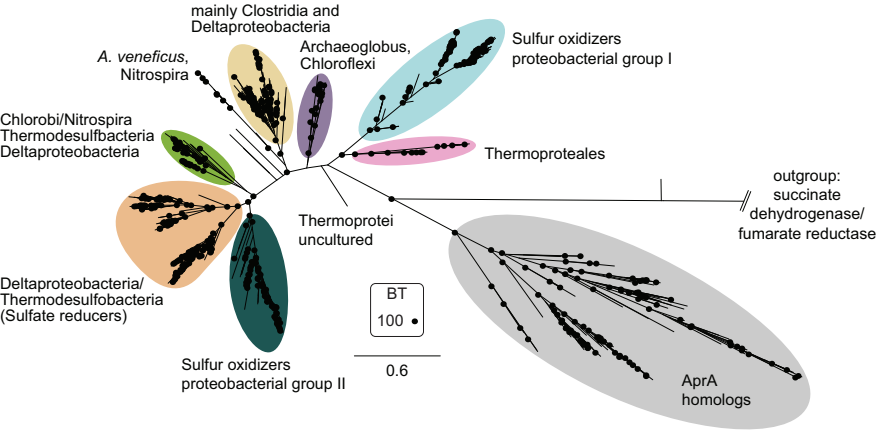
\*\* high quality metagenome (>90% completeness, <5% contamination)

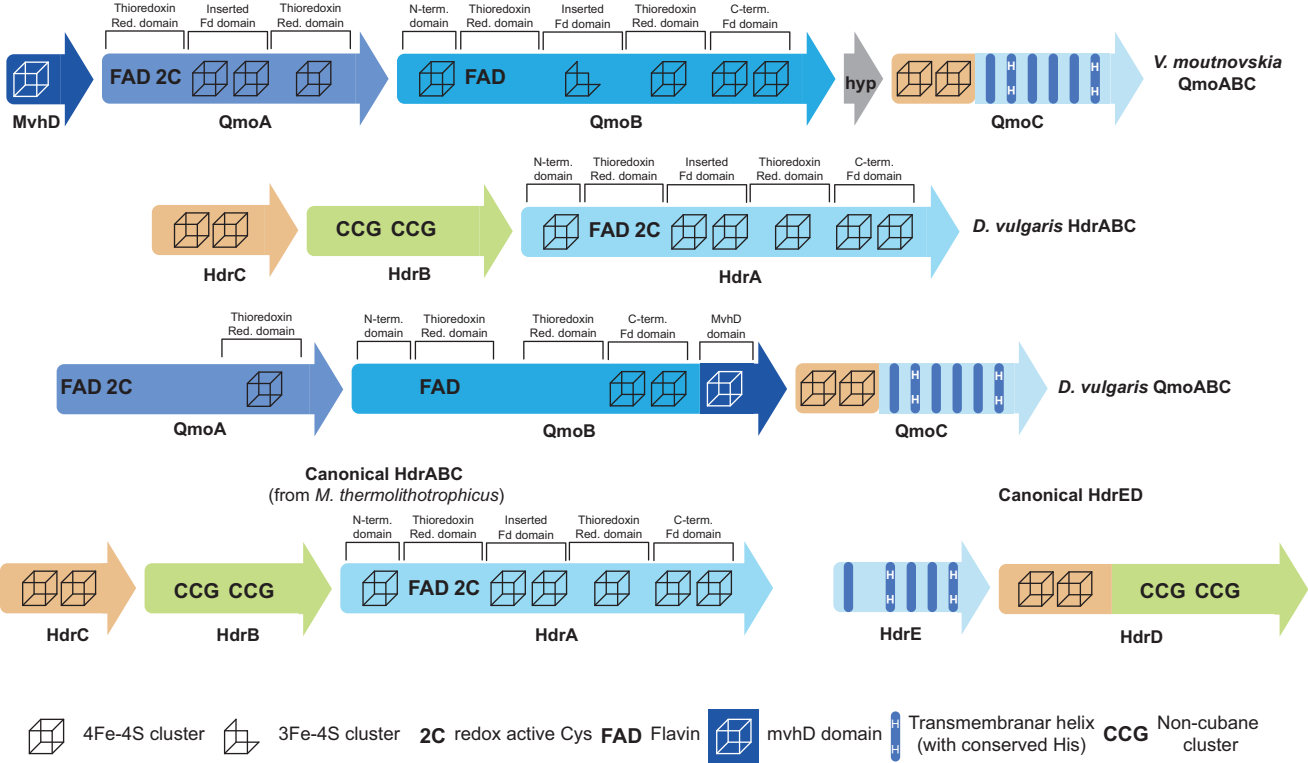
\* medium to low quality metagenome

● gene present

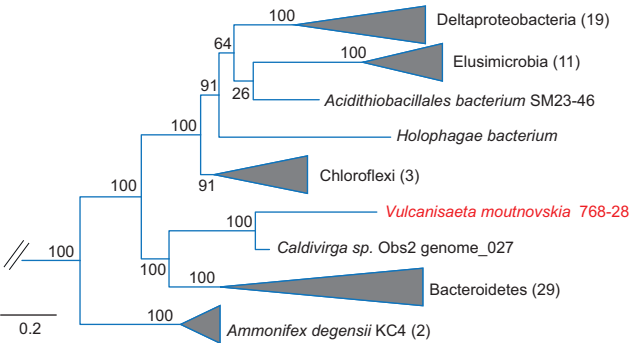
○ homologue

◐ frameshifted gene

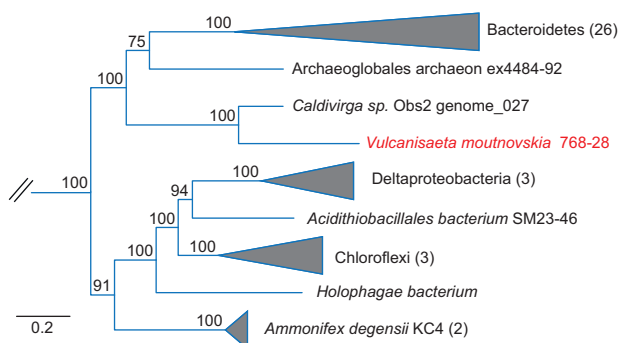


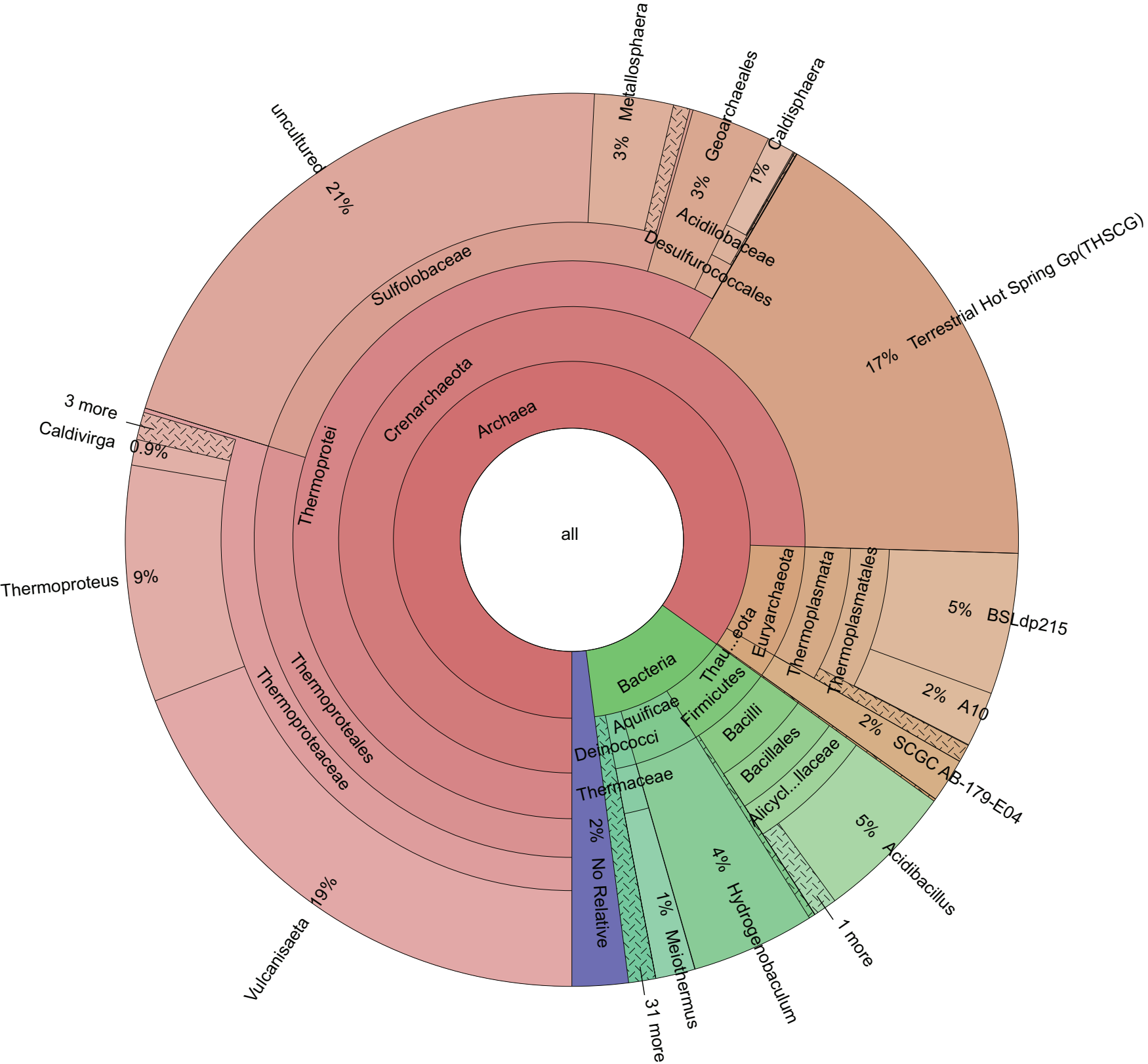


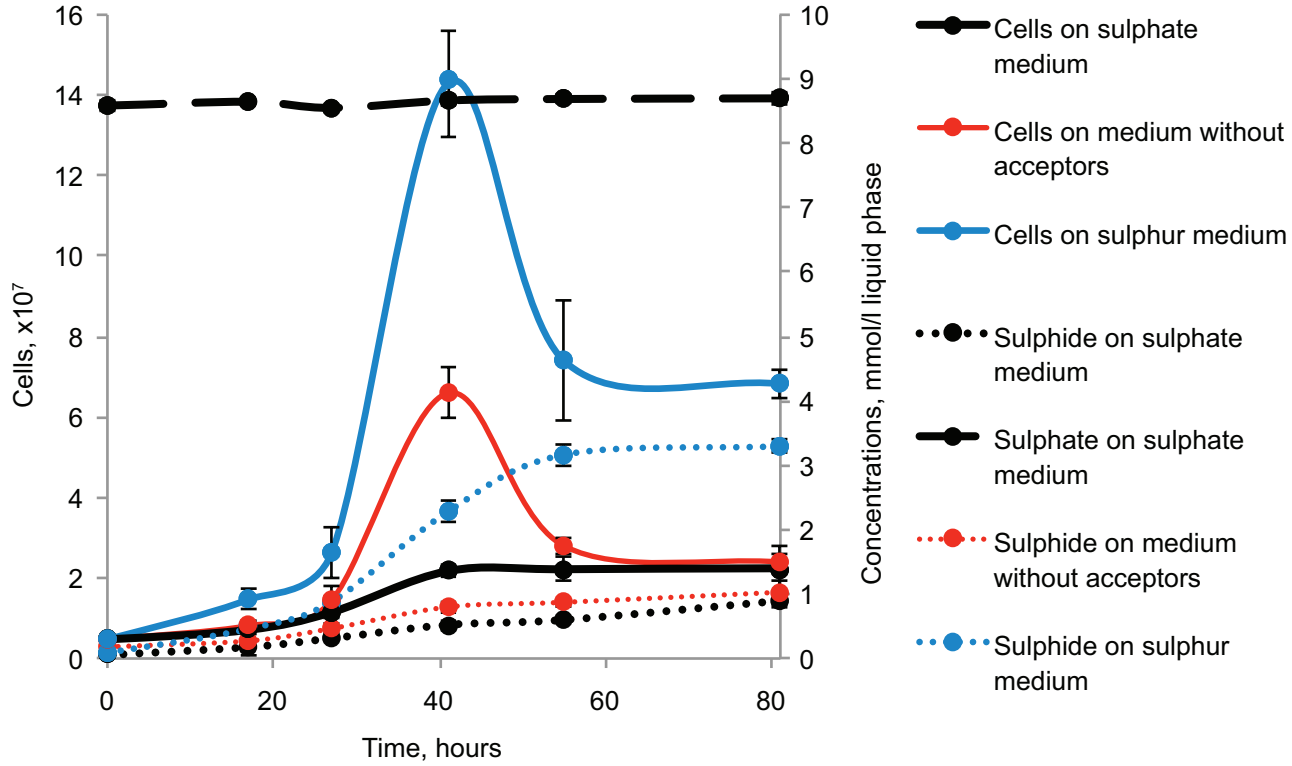
a

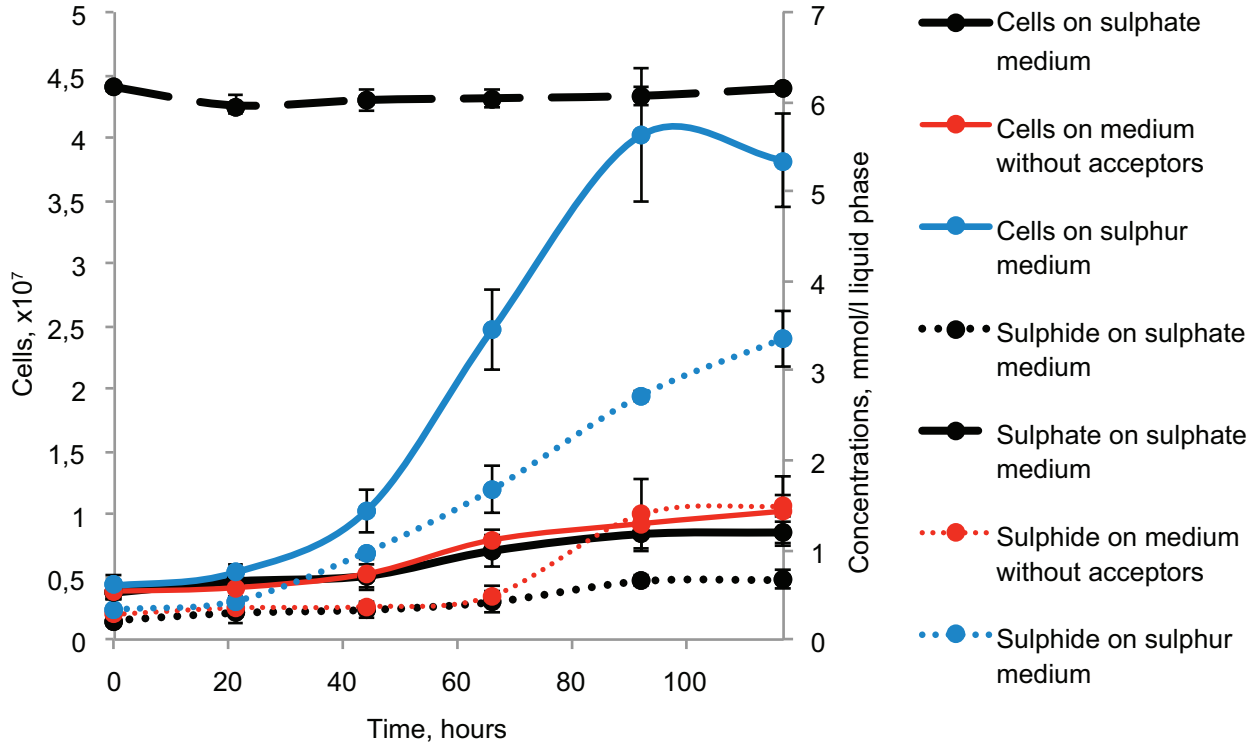


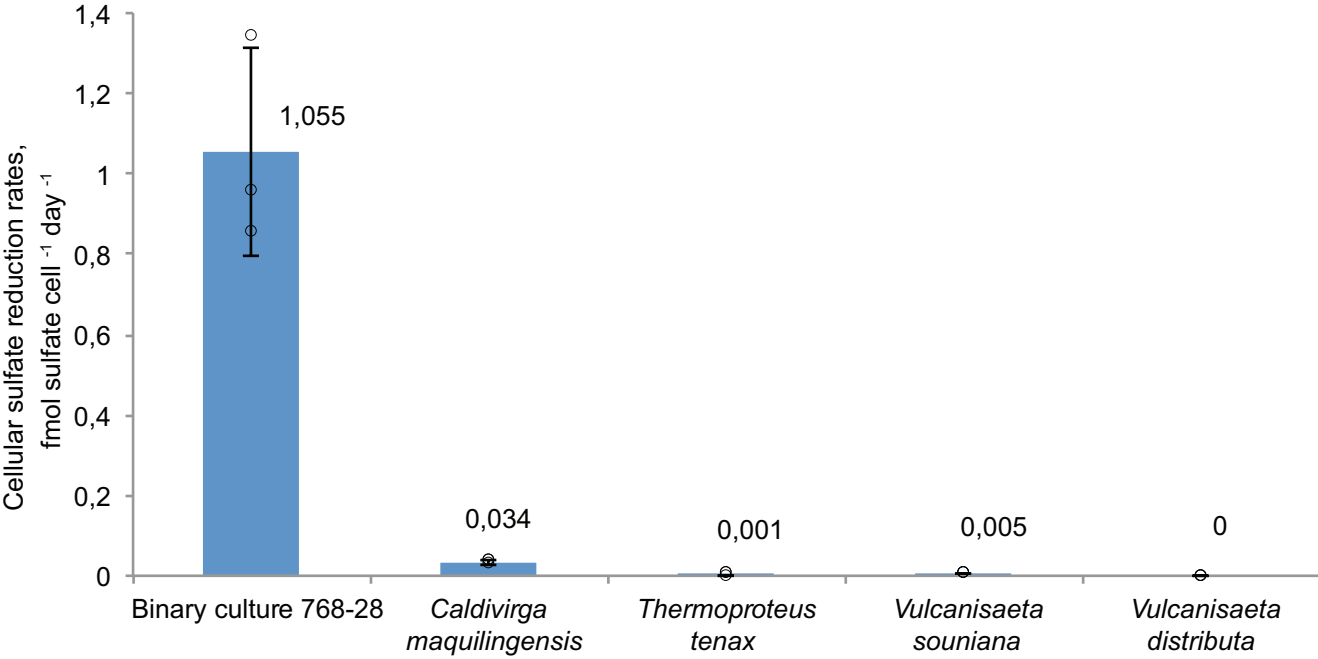
b

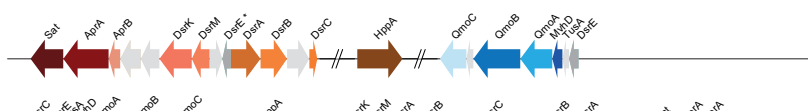
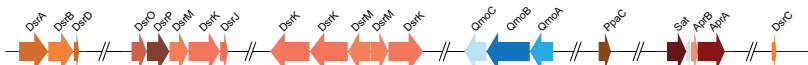
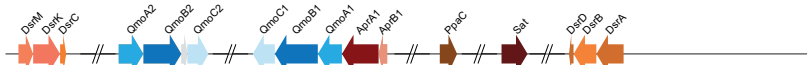
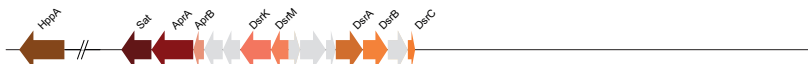
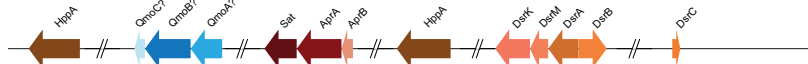






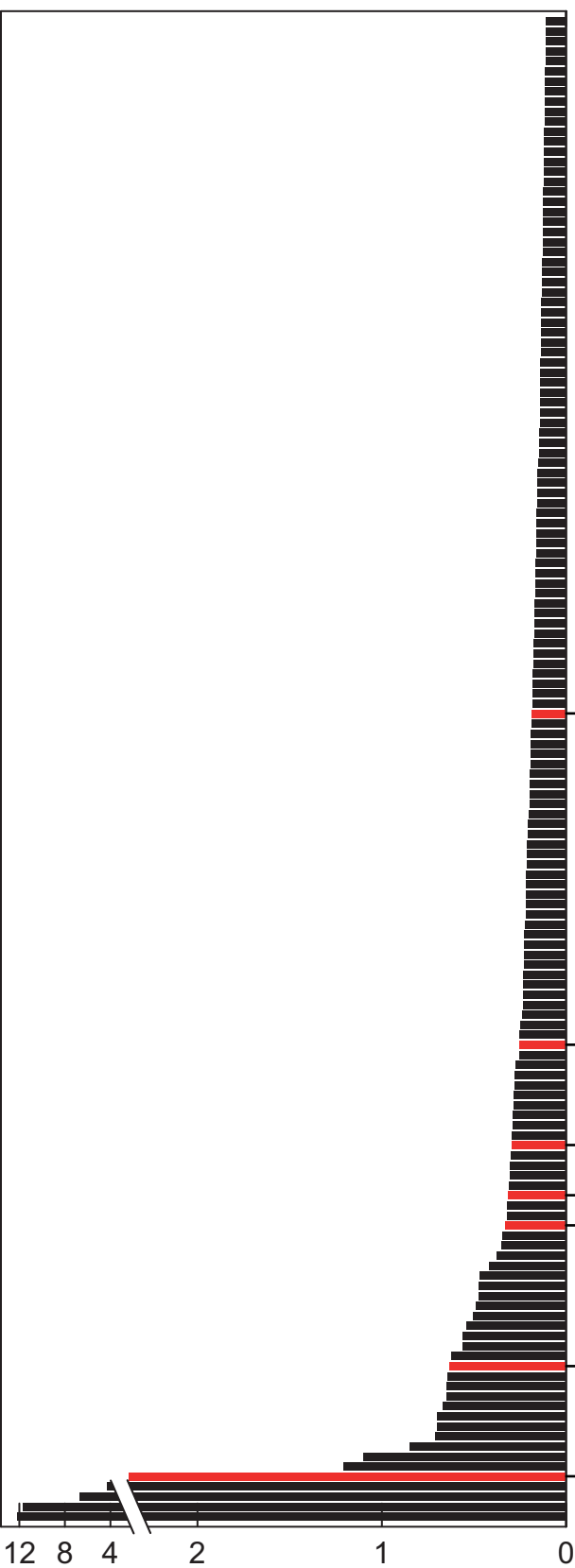
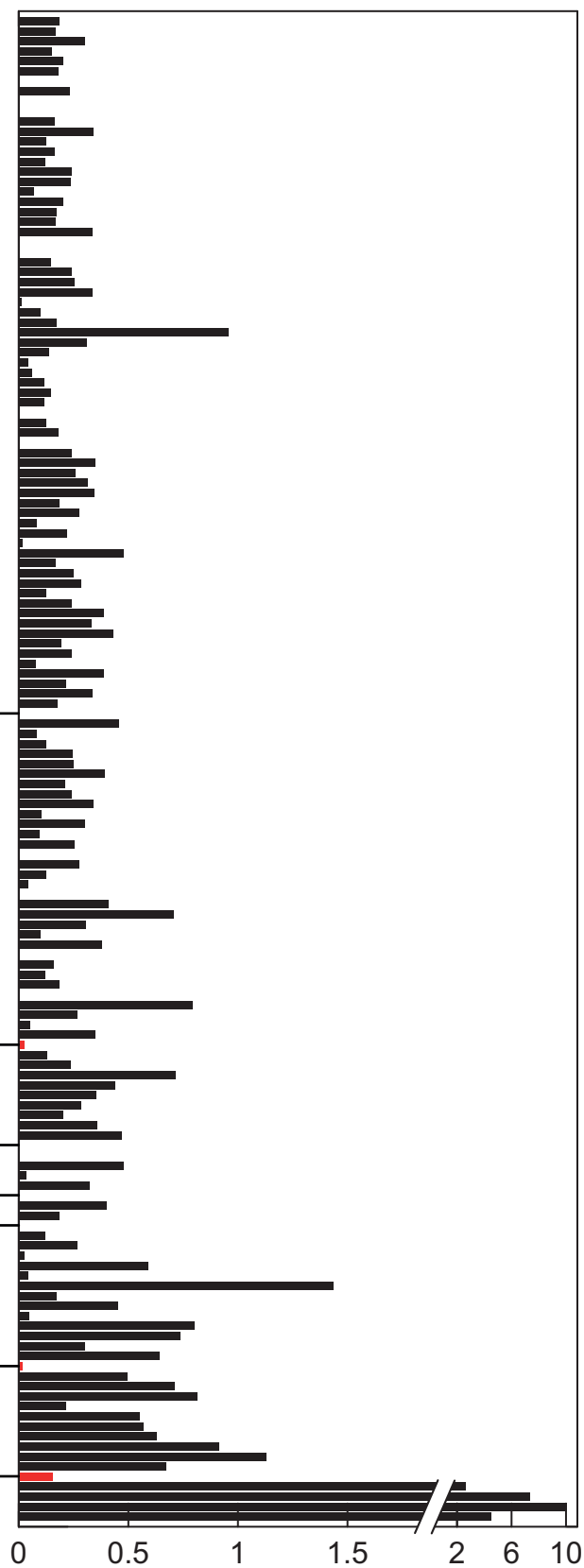


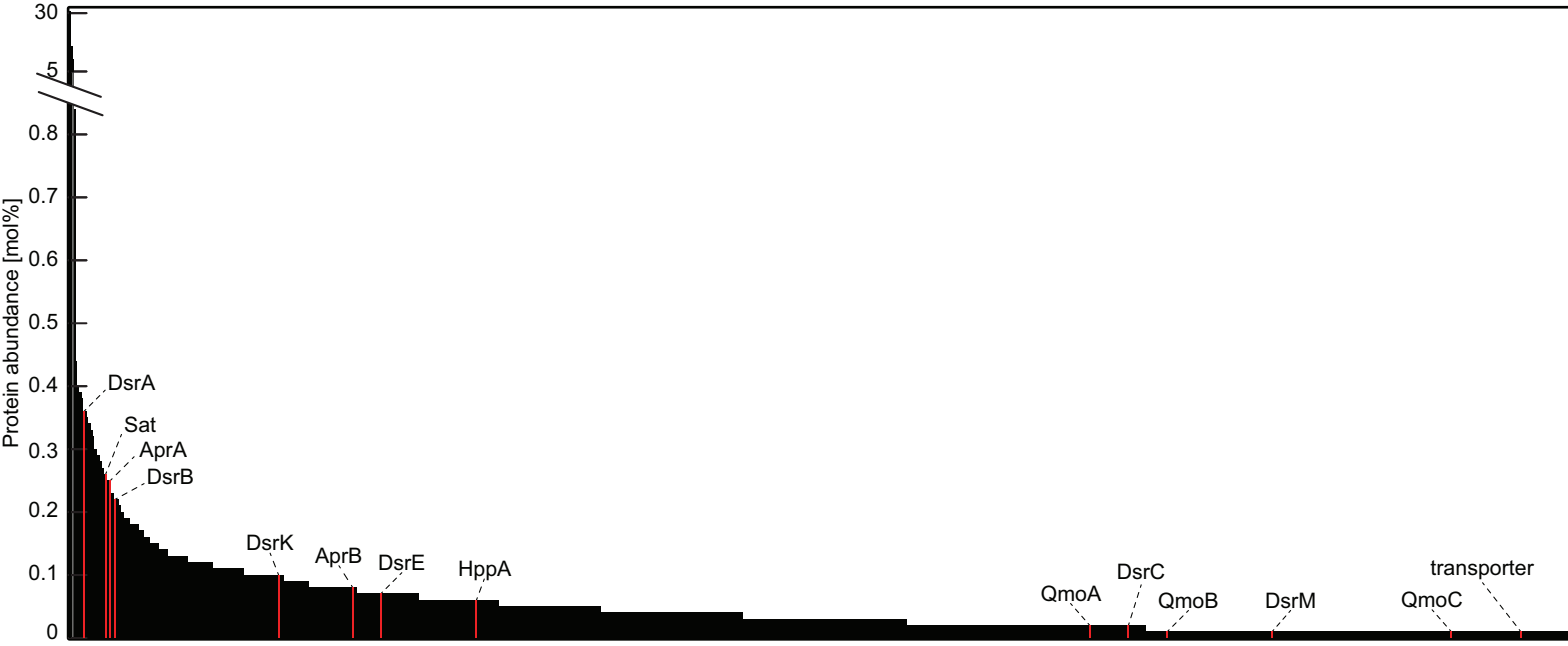


**Sulfate reducers***Vulcanisaeta moutnovskia* 768-28*Caldivirga* sp. Obs2 genome 027*Desulfovibrio vulgaris* str. Hildenborough*Archaeoglobus fulgidus* DSM 4304*Ammonifex degensii* KC4**Sulfite reducers***Vulcanisaeta distributa* DSM 14429*Vulcanisaeta souniana* JCM 11219*Caldivirga* sp. MU80*Ca. Methanodesulfokores washburnensis* MDKW

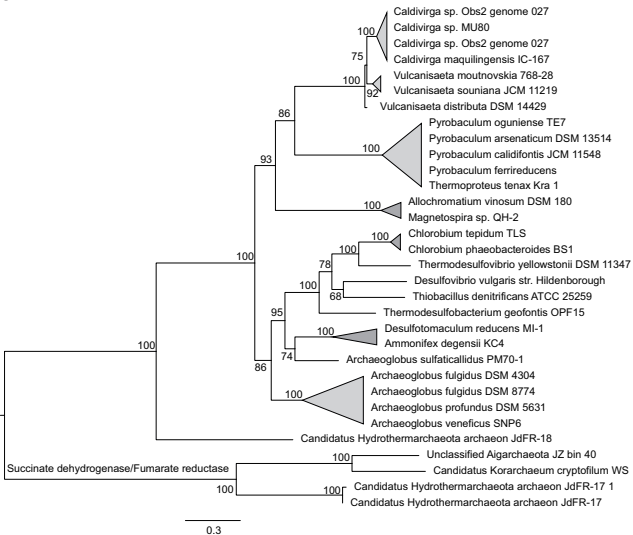
Unclassified Aigarchaeota JZ bin 15



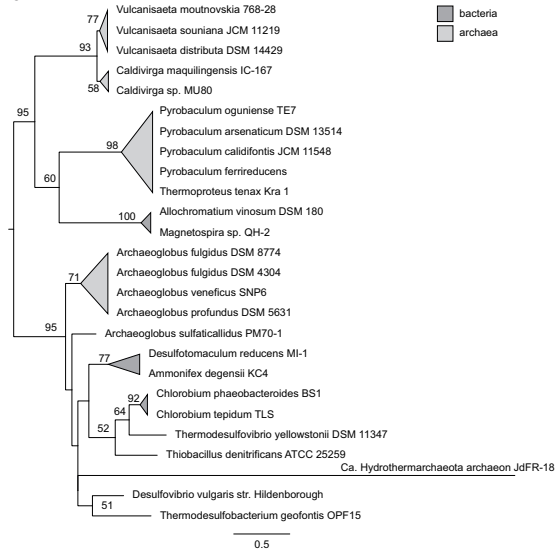
**a****b**

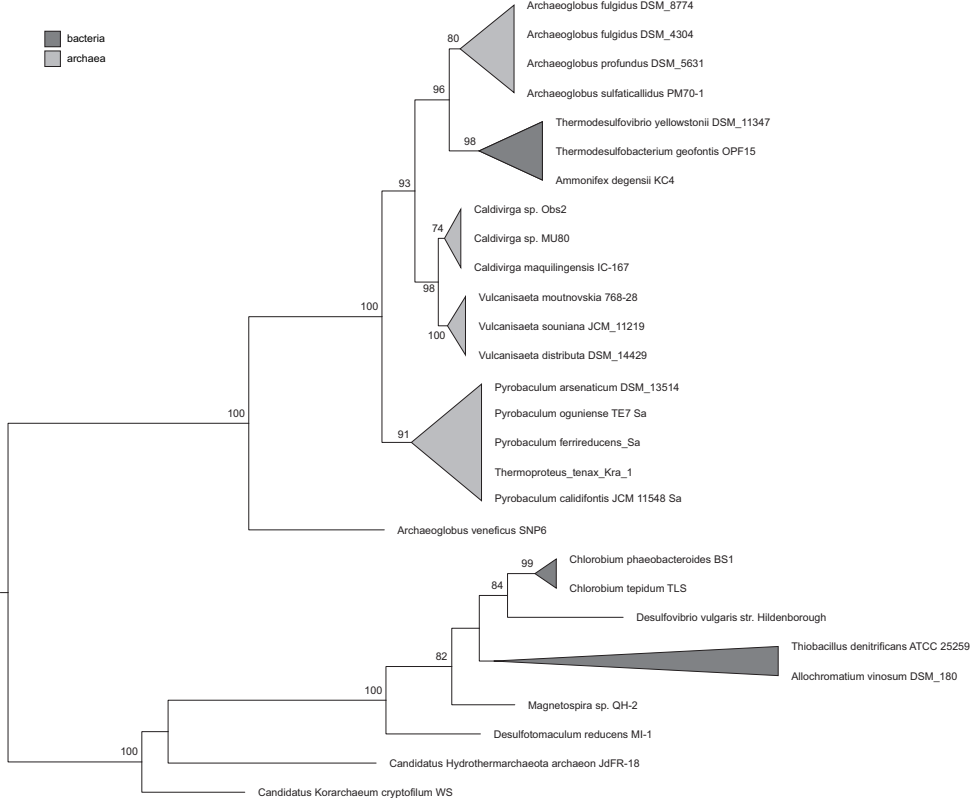


a



b





0.4

